NIH Public Access
Author Manuscript
Ann Neurol. Author manuscript; available in PMC 2016 January 01.

Published in final edited form as:
Ann Neurol. 2015 January ; 77(1): 15–32. doi:10.1002/ana.24294.

Mutual exacerbation of PGC-1α deregulation and α-synuclein oligomerization

Judith Eschbach[1,8], **Björn von Einem**[1], **Kathrin Müller**[1], **Hanna Bayer**[1], **Annika Scheffold**[2], **Bradley E. Morrison**[3], **K. Lenhard Rudolph**[4], **Dietmar R. Thal**[5], **Anke Witting**[1], **Patrick Weydt**[1], **Markus Otto**[1], **Michael Fauler**[6], **Birgit Liss**[6], **Pamela J. McLean**[7], **Albert R. La Spada**[3], **Albert C. Ludolph**[1], **Jochen H. Weishaupt**[1], and **Karin M. Danzer**[1,*]

[1]Department of Neurology, Ulm University, Albert-Einstein-Allee 11, 89081 Ulm, Germany

[2]Department of Internal Medicine III, Ulm University, Albert-Einstein-Allee 23, 89081 Ulm, Germany

[3]Department of Pediatrics, University of California, San Diego, La Jolla, CA 92093, USA

[4]Leibniz Institute for Age Research, Beutenbergstr. 11, 07745 Jena, Germany

[5]Department of Pathology, Ulm University, Helmholtzstrasse 8/1, 89081 Ulm, Germany

[6]Institute of Applied Physiology, University of Ulm, Ulm, Germany

[7]Mayo Clinic, Jacksonville, Florida, USA

[8]Inoviem scientific, 8 allée Gaspard Monge, 67083 Strasbourg, France

Abstract

Objectives—Aggregation of α-synuclein (α-syn) and α-syn cytotoxicity are hallmarks of sporadic and familial Parkinson's disease (PD) with accumulating evidence that prefibrillar oligomers and protofibrils are the pathogenic species in PD and related synucleinopathies. Peroxisome proliferator-activated receptor γ (PPARγ) co-activator 1α (PGC-1α), a key regulator of mitochondrial biogenesis and cellular energy metabolism, has recently been associated with the pathophysiology of PD. Despite extensive effort on studying the function of PGC-1α in mitochondria, no studies have addressed whether PGC-1α directly influences oligomerization of α-syn or whether α-syn oligomers impact PGC-1α expression.

Results—In this study, we found that both PGC-1α reference gene (RG-PGC-1α) and the CNS specific PGC-1α (CNS-PGC-1α) are downregulated in human PD brain, in A30P α-syn transgenic animals, and in a cell culture model for α-syn oligomerization. Importantly, down-regulation of both RG-PGC-1α and CNS-PGC-1α in cell culture or neurons from RG-PGC-1α deficient mice leads to a strong induction of α-syn oligomerization and toxicity. In contrast, pharmacological activation or genetic overexpression of RG-PGC-1α reduced α-syn oligomerization and rescued α-syn mediated toxicity.

*Corresponding author: Prof. Dr. Karin M. Danzer, Department of Neurology, Ulm University, Albert Einstein Allee 11, 89081 Ulm, Germany, Karin.danzer@uni-ulm.de.

Potential Conflict of Interest
The authors declare no direct conflicts of interests in the results of this research.

NIH-PA Author Manuscript
NIH-PA Author Manuscript
NIH-PA Author Manuscript

NIH-PA Author Manuscript

NIH-PA Author Manuscript

NIH-PA Author Manuscript

Interpretation—Based on our results, we propose that PGC-1α downregulation and α-syn oligomerization from a vicious circle thereby influencing and/or potentiating each other. Our data indicate that restoration of PGC-1α is a promising approach for development of effective drugs for the treatment of PD and related synucleinopathies.

Keywords

PGC-1α; alpha synuclein oligomers; aggregation; Parkinson's disease

Introduction

Parkinson's disease (PD) is an adult onset neurodegenerative disease characterized by α-synuclein (α-syn) neuropathology and progressive neuronal loss in the *substantia nigra pars compacta* (SN). The α-syn neuropathology spreads besides the SN widely also to other brain areas, e.g. large parts of the peripheral autonomic nervous system in early stages or the cerebral cortex in later stages [1]. The characteristic α-syn immunoreactive inclusions are termed Lewy bodies or Lewy neurites and contain fibrillar aggregates of α-syn as a main component[2]. A recent growing body of evidence, however, suggests that prefibrillar oligomers are the key contributors to the development of PD [3–7]. A-syn oligomers and prefibrillar forms, rather than mature fibrils, have recently been shown to induce cell death *in vitro* [8] and *in vivo* [9] and are thus regarded as the pathogenic species in PD [10–13]. Little is known about how and why α-syn oligomers are forming. Reactive oxygen species (ROS) increase α-syn oligomer formation, and mitochondrial alterations [14–16], leading to further increased ROS production, are associated with degeneration of midbrain dopamingergic neurons [17]. PD pathogenesis is intricately linked to mitochondrial dysfunction and oxidative stress [18–20]. Inhibiting complex I of the mitochondrial respiratory chain in dopaminergic neuronal cells reproduces many features of PD including α-syn inclusions in rats [21]. Administration of MPTP also targeting mitochondrial complex I causes acute and permanent PD in humans [22] and has been used to generate experimental models of PD in animals and in cell culture studies [23–25]. Several studies demonstrated that genes regulating mitochondrial function or oxidative stress influence the risk of PD [26–28]. One of the major regulators of mitochondrial biogenesis and energy metabolism in cells is the peroxisome proliferator-activated receptor γ (PPARγ) co-activator 1α (PGC-1α) [29]. PGC-1α controls oxidative phosphorylation, antioxidant defense [30] and autophagy[31]. Recent studies identified different tissue-specific isoforms of PGC-1α, including muscle-specific and CNS-specific isoforms (CNS-PGC-1α) [32, 33]. The reference gene of PGC-1α (RG-PGC-1α) has been reported as an important key player in several neurodegenerative diseases [34]. Restoration of PGC-1α expression ameliorates the symptoms in a mouse model of Huntington's disease (HD) by promoting the elimination of huntingtin aggregates [31]. Additionally, several studies pointing to PGC-1α as a modifier of HD [35–38], however, there is also one study questioning this association [39]. Moreover, transgenic overexpression of PGC-1α in mice improves motoneuron function and extends life span in the SOD1-G93A mouse model of ALS [40, 41]. In line with these studies, we have previously shown that RG-PGC-1α deficiency leads to an earlier age of onset and shortened survival in ALS male mice[42]. Only a few studies have addressed PGC-1α in the context of PD, and its relevance for PD is poorly understood. Genes that are regulated by PGC-1α are underexpressed in PD brains [43]; however, whether

NIH-PA Author Manuscript

NIH-PA Author Manuscript

NIH-PA Author Manuscript

RG-PGC-1α itself or CNS-PGC-1α are deregulated in PD, i.e. expressed above or below a physiological range, is not known thus far. A tight regulation of PGC-1α in the nigrostriatal system has been shown to be crucial for maintenance of dopaminergic neurons under physiological conditions[44]. In mice, repression of PGC-1α kills dopaminergic neurons, and PGC-1α activation can prevent this loss [45]. Interestingly, α-syn is able to reduce PGC-1α expression by direct interaction with its promoter [46], and PGC-1α restoration improves survival of neurons overexpressing the mutated α-syn [47]. Together, existing data from the literature point to a vicious circle between PGC1α dysfunction and α-syn oligomerizatin and toxicity. To test the hypothesis that PGC1α dysfunction and α-syn oligomerization influence each other and/or built a vicious circle we set out to determine how PGC-1α affects α-syn mediated toxicity, and more importantly, whether PGC-1α impacts α-syn oligomerization. Vice versa, we examined whether α-syn oligomers could influence RG-PGC-1α or CNS-PGC-1α expression. To address these questions, we used human PD patient material, a mouse model for PD, and a PD cell culture model to determine whether different isoforms of PGC-1α were deregulated in PD. Furthermore, using an α-syn protein complementation assay, we explored whether PGC-1α directly influences α-syn oligomer formation and α-syn-mediated toxicity.

Methods

Human Samples

Fresh frozen human brain tissue from the *substantia nigra pars compacta* was used for the determination of mRNA-levels of RG-PGC-1α and CNS-PGC-1α. All PD patients were diagnosed using the UK PD Society Brain Bank clinical diagnostic criteria at specialized centers for PD. Neuropathological diagnosis demonstrated the presence of Lewy body pathology in the *substantia nigra* with typical pathological features[1]. We used SN tissue from cases with Braak stage 5 and 6. In PD Braak stage 5, the lesions advance from the temporal mesocortex to adjacent high-order sensory association areas of the neocortex. In PD Braak stage 6, the neocortical pathology proceeds further, i.e., into the first order sensory association areas of the neocortex and, sometimes, into the neocortical primary sensory and motor fields [1]. The brain samples were received from the brain bank of Ulm University, University of California, San Diego, and the Mayo Clinic, Jacksonville, Florida. All human experiments were performed in accordance with the declaration of Helsinki and approved by the respective Local Research Ethics Committees.

Animals

Thy-1 (A30P) α-synuclein mice [48, 49] genotyping was performed as described previously [48, 49]. Mice were maintained in a temperature- and humidity-controlled environment at 23°C with a 12h light/dark cycle and had food and water *ad libitum*. Thy-1 α-syn A30P mice were repeatedly tested for α-syn expression on mRNA level and protein level. Moreover, the typical phenotype including impaired balance, hind limb clasping and a reduced position reflex as described earlier [49–51] was observed in our mice starting at 16 month of age. As an additional quality control for our mouse cohort, proteinase K PET blots (as described previously [49]) confirmed α-syn pathology beginning with the age of 12 month with inter-individual variation. Most importantly, the α-syn pathology was consistently seen

NIH-PA Author Manuscript

NIH-PA Author Manuscript

NIH-PA Author Manuscript

in Thy-1 α-syn A30P mice with the age of 18 month (data not shown). For biochemical analysis, animals were sacrificed and tissues were quickly dissected, frozen in liquid nitrogen and stored at −80°C until use. RG-PGC-1α deficient mice used in this study were described earlier [52].

Plasmids

Plasmids used in this study such as fusion constructs α-syn -hGLuc1 (S1) and α-syn -hGLuc2 (S2) as well as PGC-1α plasmid have been described previously [53–55]. Lentiviral vectors used the human p6IPZ Library from Open Biosystems. Therefore the target sequences were designed by using an algorithm approach (ShPGC-1α-A: TGCTGTTGACAGTGAGCGCGCCAACACTCAGCTAAGTTATTAGTGAAGCCACAG ATGTAATAACTTAGCTGAGTGTTGGCTTGCCTACTGCCTCGGA; ShPGC-1α-B: TGCTGTTGACAGTGAGCGACGTGTGATTTATGTCGGTAAATAGTGAAGCCACAG ATGTATTTACCGACATAAATCACACGGTGCCTACTGCCTCGGA).

Primary cortical neuron cultures

Primary cortical neurons were cultured from E16 embryos issued from a cross between two homozygous RG-PGC-1α knock-out or wildtype mice. After mechanical dissociation, cells were resuspended in Neurobasal (NB) (Gibco, Darmstadt, Germany) medium supplemented with 10% fetal bovine serum, 2 mM Glutamax, 100 U/mL penicillin, and 100 μg/mL streptomycin and plated at a density of 3.84×10^4 cells/well on 96w plates (Corning, NY, USA), 60 mm dishes at a density of 3.6×10^6 cells/dish (Costar, Corning, NY, USA) coated with 20μg/mL poly-D-lysine (Sigma-Aldrich, St. Louis, MO, USA). After 2 h medium was changed into NB/B-27 [NB medium containing 2% (v/v) B-27 supplement], 100 U/mL penicillin, 100 μg/mL streptomycin, and 2 mM/L glutamine and grown at 37°C in 5% CO_2. Medium was changed every third day partially. Neurons were grown for 4–5 days in vitro (DIV) before infected with AAV8-S1/AAV8-S2 or treated with conditioned media from S1/S2 transfected H4 cells.

Cell culture and transfection

Human H4 neuroglioma cells (HTB-148 - ATCC, Manassas, VA, USA) were maintained in DMEM medium supplemented with 10% fetal bovine serum (both from Invitrogen) and incubated at 37°C, 5% CO_2. Cells were plated 24 hours prior transfection at confluency of 80–90%. Transfection was performed using Superfect (Qiagen, Chatsworth, CA, USA) using equimolar ratios of plasmids according to the manufacturer's instructions.

Pharmacological treatments and synuclein-reuptake experiments

H4 cells were plated into 96 well plates (Costar, Corning, NY, USA) and transfected as described above. Transfection mix was incubated for 2h according to manufacturer's protocol, after 14h media was replaced by fresh culture media containing resveratrol, AICAR or compound C (Sigma-Aldrich) at the indicated concentration. After 24h post transfection α-syn oligomerization was measured using Gaussia luciferase protein-fragment complementation assay or toxicity was assessed using Caspase 3/7 activity assays (Promega, Madison, WI) (see below).

NIH-PA Author Manuscript

NIH-PA Author Manuscript

NIH-PA Author Manuscript

For bafilomycin A1 (BAF A1) experiments H4 cells were transfected as described above. After 28h post transfection 200 nM BAF A1 or DMSO control was added to the cells for another 20h before α-syn oligomerization was measured using the Gaussia luciferase protein-fragment complementation assay.

For re-uptake experiments conditioned media from S1/S2 transfected H4 cells was collected 48 hours post-transfection and centrifuged for 5 min at 3000 g to eliminate floating cells before being transferred to naïve primary neuron for the indicated time. Primary neurons were treated with a 1:1 ratio of conditioned media containing α-syn oligomers and neuronal culture media.

Toxicity assay

Toxicity was analyzed 1–2 days after S1/S2 transfection or after treatment with conditioned media from S1/S2 transfected H4 cells by using either the ToxiLight BioAssay Kit (Lonza, Rockland, ME), which quantitatively measures the release of adenylate kinase (AK) from damaged cells (Miret, 2006) or by using Apo- ONE homogeneous Caspase-3/7 assay (Promega, Madison, WI) measuring the activity of Caspases 3 and 7 using a fluorometric substrate Z-DEVD-Rhodamine 110 according to the respective manufacturers' instructions. Viability was evaluated by using the CellTiter-Glo® Luminescent Cell Viability Assay (Promega, Madison, WI), which quantifies the amount of ATP, an indicator of metabolically active cells.

Gaussia luciferase protein-fragment complementation assay

H4 cells were transfected with S1 and S2 in a white 96-well plate as described above. 24h after transfection, culture media was removed and cells were washed with PBS and placed in OPTI-MEM (Gibco, Darmstadt, Germany) for measurement. Luciferase activity from protein complementation was measured for conditioned media and live cells in an automated plate reader (Perkin-Elmer, Waltham, Massachusets) at 480 nm following the injection of the cell permeable substrate, coelenterazine (20 μM) (Prolume Ltd, Pinetop, AZ) with a signal integration time of 2 seconds.

AAV vectors construction and production

The viral vectors rAAV-CBA-SYNUCLEIN-LUC1-WPRE (S1) and rAAV-CBA-SYNUCLEIN-LUC2-WPRE (S2) used in this study were described previously [53, 54].

Lentiviral production

Lentivirus was produced in 293T HEKcells after transfection of 15 μg shRNA plasmid, 10μg HIV-gag/pol and 5 μg VSVG glycoprotein using Calcium-phosphate method in DMEM supplemented with 10% FCS in 10cm dishes. After 8h-12h transfection, cells were washed in PBS and fresh cell culture media containing DMEM with 10% FCS was added. Supernatants were harvested after 24h and 48h and filtrated through 0.22 mm filters. Human H4 neuroglioma were plated in 10cm-dishes and infected using 50% supernatant lentiviral particles and culture medium containing 8 μg/mL polybrene. After approximately 10 hours of incubation, cells were washed in PBS and medium was changed to fresh complete medium. Two days post-transduction, cells were placed into fresh complete medium

NIH-PA Author Manuscript

NIH-PA Author Manuscript

NIH-PA Author Manuscript

containing 1 μg/mL puromycin for four days. Selection medium containing 1 μg/mL puromycin was changed every two days. Efficiency of the transduced cultures, i.e., percentage of GFP expressing cells was estimated using flow cytometry analysis (FACS), and gene knockdown was evaluated by quantitative PCR. After puromycin selection, cells were counted and plated at the density of 500 cells per well into 12-well plates.

RT-qPCR

Total RNA was extracted using RNeasy Mini Plus Kit (Qiagen, Hamburg, Germany) in accordance with the manufacturer's instructions. Briefly, cell cultures were disrupted directly into the buffer RLT (Qiagen, Hamburg, Germany) supplemented with 10% β-mercaptoethanol (Sigma-Aldrich, Taufkirchen bei München, Germany). For RNA extraction from tissue, frozen tissues were placed into a tube containing a 5 mm stainless steel bead. Working on ice, 700μL of buffer RLT supplemented with 10% β-mercaptoethanol was added, and homogenisation was performed in a TissueLyser (Qiagen, Valencia, CA) at 30 Hz for 3 min. After RNA extraction, RNA concentration was measured using a nanodrop (ThermoScientific, Waltham, MA) and 1 μg of total RNA was used to synthesize cDNA using I-script reverse transcriptase (Bio-Rad Laboratories, München, Germany) containing oligo-dT primers and random primers. cDNA were then diluted 10 times and PCR analysis was performed on a Bio-Rad iCycler System using iQSYBR Green Supermix (Bio-Rad Laboratories, München, Germany). A specific standard curve was performed in parallel for each gene to assess the specificity of the products, for quantification of the respective transcripts in duplicate. PCR conditions were 3 min at 94°C, followed by 40 cycles of 45 s at 94°C and 10 s at 60°C. The relative level of each RNA was normalized to the two housekeeping genes polymerase (RNA) II polypeptide A (POLR2A II) and TATA box binding protein (TBP). These housekeeping genes have been thoroughly validated and turned out to be extremely stable in our previous studies [42, 56, 57]. The CFX Manager™ Software was used to analyze our data. Briefly, relative quantification was achieved by calculating the ratio between the cycle number (Ct) at which the signal crossed a threshold set within the logarithmic phase of the gene of interest and that of genes used for normalization calculated by the relative quantity of the reference genes.

CNS- and RG-specific *Ppargc1a* transcripts were quantified using primers targeting CNS-specific exons B1 and B4 [33] or exons 1 and 2, respectively. PGC-1β transcripts were quantified using PGC-1β-specific primers. Human primers: PGC-1α B1/B4: forward-TACAACTACGGCTCCTCCTGG, reverse-TACCCTTCATCCATGGGGCTC; PGC-1α Ex1/Ex2: forward-CTTGGGACATGTGCAGCCAAG, reverse-GCTGTCTGTATCCAAGTCAT; PGC-1 β: forward-AAATCTCAAGGGGAGCGTGG, reverse-AGATGCTCCAAGCCAATGCT; Polymerase II: forward-TTGTGCAGGACACACTCACA, reverse-CAGGAGGTTCATCACTTCACC; TBP: forward-CCCATGACTCCCATGACC, reverse-TTTACAACCAAGATTCACTGTGG; TFAM: forward-AAGCTCAGAACCCAGATGCAA, reverse-CAGGAAGTTCCCTCCAACGC; TFEB: forward-ACCCTGAGAGGGAGTTGGAT, reverse-GGCATCTGCATTTCAGGATT. Mouse primers: PGC-1α B1/B4: forward-TACAACTACGGCTCCTCCTGG, reverse-TACCCTTCATCCATGGGGCTC; PGC-1α: forward-AGAGTGTGCTGCTCTGGTTG, reverse-TTCCGATTGGTCGCTACACC;

NIH-PA Author Manuscript

NIH-PA Author Manuscript

NIH-PA Author Manuscript

Polymerase II: forward-GCTGGGAGACATAGCACCA, reverse-TTACTCCCCTGCATGGTCTC; TBP: forward-GGCGGTTTGGCTAGGTTT, reverse-GGGTTATCTTCACACACCATGA.

A linear mixed effects model for estimating disease, age, gender and PMI effects

Similar to the method from Schlaudraff et al. [58] we have applied a linear mixed effects model analysis on our gene expression data. This allowed us to estimate possible confounding effects by covariates like age, gender and post-mortem interval (PMI). The following model was fit to the natural logarithm of relative expression data for RG-PGC-1α (formula in Wilkinson notation [59]):

$$log(PGC1\alpha_{RG}) \sim 1 + group + sex + age + PMI + (1|batch)$$

Herein the *group* effect represents *control* or *PD* and *sex* the gender (*male* or *female*). Random effects were introduced on the intercept to calibrate for differences between different batches of samples that were measured on different PCR-plates. The analysis was performed with the *LinearMixedModel* class of the Statistics Toolbox for Matlab V8.2 (The MathWorks, Inc., Natick, MA, USA) which fitted the model by likelihood maximization.

Western blotting

Cells or human brain tissue were lysed in RIPA buffer (150 mM NaCl, 1.0% IGEPAL, 0.5% sodium deoxycholate, 0.1% SDS, and 50 mM Tris, pH 8.0 and protease inhibitor cocktail 1 tablet/10 mL (Roche Diagnostics, Mannheim, Germany). Protein quantification was carried out using a BCA assay kit (ThermoScientific, Bonn, Germany). Equal amounts of soluble proteins were denatured by boiling, resolved by 9% sodium dodecyl sulfate polyacrylamide gel electrophoresis (SDS- PAGE). After transfer to nitrocellulose membrane (Protran, Schleicher and Schuell, Whatman GmbH, Dassel, Germany) membranes were blocked with 10% non-fat dry milk in TBS-T for 30 min at room temperature. Membranes were then incubated with primary antibodies (mouse anti-α-syn, 1:1000, BD Transduction, Heidelberg, Germany; mouse anti-actin: monoclonal, 1:500, cell signaling, Frankfurt am Main, Germany, home-made rabbit anti-PGC-1α, 1:500, Eurogentec, Köln, Germany) overnight at 4°C. After three 5–10 min TBS-T washes, membranes were incubated at room temperature for 1 hour with horse radish peroxidase (HRP)-conjugated secondary antibody (anti mouse; 1:10 000, Invitrogen, Freiburg, Germany). After three 5– 10 min TBS-T washes, immunoblots were analyzed using ECL chemiluminescent detection system (Amhersham/GE HealthCare, Buckinghamshire, UK). Densitometric quantification was performed using ImageJ software (http://rsb.info.nih.gov/ij/).

Autophagosome detection

The Premo Autophagy Sensor Kit (Invitrogen) was employed for autophagosome detection, according to the guidelines. Briefly, H4 cells were transfected with the indicated constructs using Superfect (Qiagen, Chatsworth, CA, USA) and 24hour after, they were transduced with BacMam LC3B-GFP with a multiplicity of infection (MOI) equal to 10, using 5×10^4 cells in 4-well Cell Culture Chambers (Sarstedt, Nümbrecht, Germany) for 24hours. An

NIH-PA Author Manuscript

NIH-PA Author Manuscript

NIH-PA Author Manuscript

inverted fluorescence microscope (Axio observer-A1, Zeiss, Göttingen, Germany) was employed for live cells imaging using 60× magnification. Quantification of autophagosome was performed using the plugging ImageJ autocounter (http://rbsweb.nih.gov/ij/) as described previously [60].

Statistical analysis

Statistical comparisons were accomplished with the unpaired Mann–Whitney–Wilcoxon for comparison of two groups or ANOVA followed by the post hoc Tukey multiple comparisons test for multiple comparisons using PRISM version 6.0 software (GraphPad, San Diego, USA).

Results

Repression of PGC-1α in Parkinson's disease patients, in vivo and in vitro models for synucleinopathies

Since PGC-1α dependent genes have been shown to be downregulated in the brains of PD patients [43], we asked whether the RG-PGC-1α itself and CNS-PGC-1α transcripts are regulated in PD. Real-time quantitative PCR (RT-qPCR) was performed in post-mortem tissue from the SN of PD patients and non-PD controls. Neuropathological diagnosis demonstrated the presence of Lewy body pathology in the SN (from patients with PD Braak stages 5 and 6; see material and methods section and Table 1). We found a reduced expression of the RG-PGC-1α by nearly 70% in the SN of PD patients (Fig 1A), whereas the CNS-PGC-1α was unchanged in the SN of PD patients (Fig 1B). Although control and PD samples were well matched with respect to age and post-mortem interval (PMI) with no significant differences (age: 72.2±3.76 vs. 74.5±1.45 years, p=0.930, PMI: 25.2±5.35 vs. 27.0±8.22 h for control and PD, respectively), a linear mixed effect model was fit to the data to further exclude possible additional confounding influences by these covariates as well as gender effects. The approach is based on Schlaudraff et al. [58] who have applied a linear mixed effects model for the analysis of single cell gene expression data. We were testing for effects on the relative expression values of RG-PGC-1α. Logarithmic transformation led to a distribution of the data that was closer to Gaussian distribution and therefore improved the fit but had no qualitative effect on the test results. Control versus PD was the only significant single effect (estimate=-0.97±0.340, p=0.011) indicating a down-regulation of RG-PGC1α in PD (Fig 2 and Supplementary Table 1). Furthermore, Western Blot analysis with a PGC-1α specific antibody that does not distinguish between RG- or CNS-PGC-1α confirmed a reduction of PGC-1α in SN of PD patients at the protein level (Fig 1C).

To gain insight into the mechanisms underlying the PGC-1α deregulation in PD, we turned to a well characterized transgenic mouse model overexpressing the human PD associated A30P α-syn mutation [48, 49]. Aggregation of α-syn is a major hallmark of PD and is recapitulated in the A30P α-syn mouse model by protease-K resistant α-syn fibrils mainly in the brain stem, midbrain and spinal cord [61]. Interestingly, we found in the brainstem of A30P α-syn mice an age-dependent decline of RG-PGC-1α and CNS-PGC-1α levels starting at 6 or 3 month of age, respectively (Fig 1D, E). To correlate PGC-1α downregulation with α-syn aggregation, we also analyzed the cortices of these mice, where

NIH-PA Author Manuscript

NIH-PA Author Manuscript

NIH-PA Author Manuscript

widespread expression of α-syn is present but there is no occurrence of fibrils. In contrast to the brainstem, where the decrease of RG-PGC-1α is already manifest at 6 months of age, RG-PGC-1α downregulation in the cortex of A30P α-syn mice starts at 15 months of age (Fig 1F) which might be related to a later onset of α-syn aggregation processes in this area. Also, for the CNS-PGC-1α isoforms, we noted a reduction in expression levels that occurred later in the cortices (6 month of age) than in the brainstem (3 month of age) (Fig 1G). Taken together, these results indicate an association between α-syn aggregation and PGC-1α downregulation.

To investigate if the presence of α-syn oligomers in cell culture has a direct effect on PGC-1α transcript levels, we expressed α-syn oligomers and quantified RG-PGC-1α and CNS-PGC-1α mRNA levels using qRT-PCR. To determine oligomeric α-syn inside cells, we used a protein-fragment complementation assay where α-syn was fused to non-bioluminescent N- or C-terminal fragments of Gaussia princeps luciferase (α-syn-hGLuc1 (S1) and α-syn-hGLuc2 (S2)) that reconstitute, when brought together by α-syn/α-syn interactions [53, 62]. The (patho) physiological validity of the α-syn protein complementation system and its comparison with non-tagged wt α-syn using multiple methods was repeatedly shown before in previous studies [53, 54, 62–64]. These constructs were used to infect wild-type primary cortical neurons with adeno-associated virus (AAV), encoding either S1 or S2. Interestingly, expression of both RG-PGC-1α and CNS-specific isoforms were decreased when α-syn oligomers are present (Fig 1H, I). A reduction of RG-PGC-1α was also detected in human neuroglioma cells H4 after co-transfection of S1 and S2 (Fig 1J). Of note, we did not observe a reduction in CNS-PGC-1α (Fig 1K) in H4 cells when co-transfected with S1 and S2, possibly because levels of CNS-PGC-1α in H4 neuroglioma cells were barely above background levels.

Collectively, RG-PGC-1α and CNS-PGC-1α deregulation in postmortem PD patient material, A30P-α-syn transgenic mice and in a cell culture models for α-syn oligomerization strongly support a link between α-syn oligomerization and deregulation of RG-PGC-1α and CNS-PGC-1α expression.

PGC-1α knockdown increases α-synuclein oligomerization

To directly link PGC-1α downregulation and α-syn oligomerization, we used lentiviral delivery of PGC-1α-shRNAs (shPGC-1α-A and ShPGC-1α-B) for reduction of both RG-PGC-1α and CNS-PGC-1α expression. We then co-transfected human H4 cells with S1/S2 constructs to measure α-syn oligomerization. Successful and specific downregulation of PGC-1α isoforms was confirmed by qRT-PCR (Fig 3 A–C) and Western blotting (Fig 3D). Interestingly, we found that RG-PGC-1α and CNS-PGC-1α silencing led to a 1.5 fold increase of α-syn oligomers (Fig 3E) while no significant differences in α-syn protein levels were detected (Fig 3F). Concurrently, knock down of PGC-1α isoforms also resulted in an increase of α-syn-mediated-toxicity (Fig 3 G, H).

To further validate the consequences of PGC-1α loss of function on α-syn oligomerization, we co-infected primary cortical neurons from both RG-PGC-1α deficient mice [52] and wild-type mice with AAV-S1 und AVV-S2 and observed 20% more α-syn oligomers in the RG-PGC-1α deficient primary neurons (Fig 4A). To exclude the possibility that the increase in

NIH-PA Author Manuscript

NIH-PA Author Manuscript

NIH-PA Author Manuscript

α-syn oligomers is due to increased expression levels in S1 and S2 in the RG-PGC-1α KO condition we performed Western Blot analysis and detected comparable levels of S1 and S2 in both conditions (Fig 4B). However, no obvious increase in cytotoxicity was seen in the PGC-1α KO condition (data not shown). Together, these findings suggest that PGC-1α deficiency can promote α-syn oligomerization.

PGC-1α ameliorates α-synuclein oligomerization

Since we observed PGC-1α down-regulation in PD brains, in α-syn transgenic mice, and in a cell culture model for α-syn oligomerization, we asked whether overexpression of PGC-1α could rescue α-syn oligomerization. Indeed, we found that co-transfection of RG-PGC-1α together with S1 and S2 dramatically reduced α-syn oligomers by approximately 50% and 70% after 24h and 36h, respectively (Fig 5A). To ensure that PGC-1α is functionally active in our conditions, qRT-PCR for the RG-PGC-1α target genes TFAM and TFEB was performed. A significant induction of TFAM and TFEB, when PGC-1α was co-transfected together with S1/S2, confirmed functionally active RG-PGC-1α (Fig 6). The observed reduction in α-syn oligomers might partially be attributed to a small trend of PGC-1α affecting α-syn protein expression, as Western Blot analysis revealed slightly reduced α-syn protein levels after 24h and 36h in the RG-PGC-1α condition compared to myc-control transfected S1/S2 H4 cells (Fig 5B). PGC-1α has been previously reported to promote the elimination of huntingtin aggregates by activating transcription factor EB (TFEB), a master regulator of the autophagy-lysosome pathway (ALP) [31]. To assess whether autophagy is involved in reduction of α-syn oligomers when PGC-1α is overexpressed, BacMam LC3B-GFP transduction was carried out. This system enables the expression of LC3B-GFP, ensuring efficient visualization of LC3 positive vesicles. LC3 staining was quantified using autophagy autocounter software, as published previously [60]. When S1/S2 was overexpressed autophagy was reduced, however, RG-PGC-1α could rescue this effect by a strong upregulation of autophagy (Fig 5C, D), suggesting that α-syn oligomers are specifically reduced due to RG-PGC-1α mediated induction of autophagy. To determine whether RG-PGC-1α is capable to rescue α-syn mediated toxicity, we measured cell viability after S1/S2 and RG-PGC-1α co-transfection. Notably, RG-PGC-1α could rescue α-syn mediated derogation in cell viability (Fig 5E). To further support the idea that the ALP might contribute to RG-PGC-1α related reduction in α-syn oligomers, H4 cells were co-transfected with S1 and S2 together with RG-PGC-1α or myc control plasmid and treated with the ALP inhibitor bafilomycin A1 (BAF A1) or DMSO. The reduction of α-syn oligomerization due to RG-PGC-1α was mainly abolished under the ALP inhibitor BAF A1 compared to the DMSO control, suggesting that an intact ALP is necessary for a RG-PGC-1α related reduction in α-syn oligomers (Fig 5F).

Collectively, these data indicate that induction of RG-PGC-1α can reduce α-syn oligomerization and related α-syn mediated toxicities.

Pharmacological modulation of PGC-1α alters α-syn oligomerization

To further validate the effect of PGC-1α on α-syn oligomerization, we chose a pharmacological approach to modulate PGC-1α activation. Resveratrol and AICAR have been described as potent PGC-1α activators [65, 66]. Resveratrol activates PGC-1α through the

NIH-PA Author Manuscript

NIH-PA Author Manuscript

NIH-PA Author Manuscript

upstream activators, Sirtuin1 and AMPK [65, 67, 68], and AICAR activates PGC-1α by promoting AMPK-mediated phosphorylation [69, 70]. We found that both resveratrol and AICAR treatments resulted in a robust decrease of α-syn oligomers after 24h treatment in S1/S2 transfected H4 cells (Fig 7A). In contrast to PGC-1α activation, treatment with the PGC-1α inhibitor compound C, which inhibits the upstream-PGC-1α activator AMPK [71], strongly promoted α-syn oligomerization (Fig 7B) without changes into S1/S2 protein contents (Fig 7C). Concurrently, we observed a reduction in cytotoxicity by resveratrol and AICAR treatment compared to DMSO control (Fig. 7D). To test, if resveratrol and AICAR reduce α-syn oligomerization truly via PGC-1α, we downregulated PGC-1α by lentiviral delivery of PGC-1α-shRNAs (shPGC-1α-A and ShPGC-1α-B) in H4 cells. We then co-transfected H4 cells with S1/S2 and treated them with resveratrol, AICAR or DMSO control. In contrast to application of scramble lenti-virus, silencing of RG-PGC-1α and CNS-PGC-1α abrogated the α-syn oligomer reducing effect of resveratrol and AICAR thus verifying that resveratrol and AICAR do not reduce α-syn oligomers in PGC-1α deficient cells (Fig. 7E).

Since resveratrol had the strongest effect on α-syn oligomer reduction in our experimental setting, we asked whether this reduction evolves over time, and thus treated S1/S2 transfected H4 cells for different time periods. Indeed, a small reduction in α-syn oligomers was found already after 6h resveratrol treatment, which progressed further over time (Fig 8A). Next we examined whether the reduction of α-syn oligomers depends on the concentration of resveratrol. Luciferase assays verified a dose-dependent decrease of α-syn oligomers under resveratrol treatment (Fig 8B). Thus, reduction of α-syn oligomers by resveratrol occurs in a time and dose dependent manner. Together, PGC-1α overexpression or PGC-1α pharmacological activation is capable to reduce α-syn oligomerization.

RG-PGC-1α deficient neurons are more vulnerable to extracellular α-syn oligomers

We and others have previously shown that exogenous addition of α-syn oligomers can induce Lewy body like pathology and related toxicities [8, 72–74]. Cell to cell transmission of pathological α-syn and spreading of α-syn pathology has been demonstrated in a number of studies [75, 76771]. To determine whether RG-PGC-1α deficient cells are more vulnerable to exogenous addition of α-syn oligomers, we treated primary neurons from WT or RG-PGC-1α deficient mice with conditioned media (CM), either containing α-syn oligomers S1/S2 or CM from mock transfected H4 cells. After 2 or 3 days incubation, we measured luciferase activity indicative of α-syn oligomers inside primary neurons. Strikingly, we found that RG-PGC-1α deficient neurons had remarkably higher levels of α-syn oligomers compared to neurons from wild-type mice after 72h incubation (Fig 9C) with a trend visible already after 24h (Fig 9A), suggesting RG-PGC-1α deficient cells are less capable to handle α-syn oligomers. Interestingly, in RG-PGC-1α deficient cells, we saw a strong increase in toxicity when treated with CM containing α-syn oligomers compared to wildtype neurons indicating a higher vulnerability of RG-PGC-1α deficient neurons to extracellular α-syn oligomer mediated toxicity (Fig 9 B, D). Thus, RG-PGC-1α deficiency potently exacerbates extracellular α-syn oligomer mediated toxicity.

NIH-PA Author Manuscript

NIH-PA Author Manuscript

NIH-PA Author Manuscript

Discussion

The present study provides the first direct evidence that PGC-1α deregulation and α-syn aggregation might form a vicious circle influencing and potentiating each other: PGC-1α reduces α-syn oligomerization and ameliorates α-syn mediated toxicity. In contrast, α-syn oligomerization is increased in RG- PGC-1α deficient neurons and neuroglioma cells where PGC-1α is knocked down via PGC-1α-shRNAs. Moreover, PGC-1α appears to be deregulated in human PD brain, in α-syn transgenic mice, and in an *in vitro* cell culture model for α-syn oligomerization further strengthening the idea that PGC-1α deregulation influences α-syn oligomer mediated toxicity and vice versa. Finally, we found that RG-PGC-1α deficient neurons are more vulnerable for extracellular α-syn oligomer mediated toxicity.

PGC-1α has been found to be widely expressed in the brain [78]. Recent studies highlight the importance of tightly controlling the expression levels of PGC-1α. Non-physiological overexpression of PGC-1α in dopaminergic neurons induces degeneration of dopaminergic neurons in the rat nigro-striatal system [44]. Cardiac overexpression of PGC-1α causes severe abnormalities in the myocyte architecture due to extensive mitochondrial proliferation [79, 80]. In the skeletal muscle, PGC-1α overexpression enhances not only mitochondrial biogenesis but also respiration uncoupling, leading to muscle atrophy [81]. In contrast, PGC-1α expression within physiological level improves insulin sensitivity in skeletal muscle [82]. Our study further underlines a critical need for maintaining physiological levels of PGC-1α activity. In contrast to excessive levels of PGC-1α, underexpression of PGC-1α might have detrimental effects on neuronal survival. We found reduced expression of RG- PGC-1α in the SN of PD patients compared to non-PD controls. Since RG- PGC-1α transcript levels were normalized to housekeeping genes POLR2A and TBP it is not likely that the reduction in RG- PGC-1α levels is solely due to neuronal loss in the SN of PD patients. The downregulation of RG-PGC-1α is completely associated with the presence of PD. Especially age and gender did not engage any relevant statistical influence on the expression level in our RG-PGC-1α data as we could demonstrate by the application of a linear mixed effects model. Interestingly, primary neuronal cultures showed reduced levels of both RG-PGC-1α and CNS-PGC-1α when α-syn oligomers were overexpressed. Our results are also in accordance with a prior study, demonstrating that genes expressed in response to PGC-1α are underexpressed in PD patients [43]. Moreover, in a transgenic mouse model overexpressing human A30P α-syn, which does not display nigral cell loss[49–51, 83], we demonstrated a down regulation of both RG-PGC-1α and CNS PGC-1α in the brainstem of transgenic mice overexpressing human A30P α-syn compared to wild-type mice, at early time points. In contrast, in the cortices of α-syn transgenic mice where widespread expression of α-syn is present, but no occurrence of pathogenic fibrils [61] RG-PGC-1α and CNS PGC-1α were deregulated at later time points indicating a link between α-syn aggregation and PGC-1α deregulation. Most importantly, down-regulation of RG-PGC-1α and CNS-PGC-1α could be modeled in cell culture using lentiviral vectors encoding small hairpin RNA directed against PGC-1α, leading to a strong induction of α-syn oligomerization and a subsequent increase in toxicity. Moreover, also neurons of RG-PGC-1α deficient mice displayed increased oligomerization of α-syn, collectively, pointing

NIH-PA Author Manuscript

NIH-PA Author Manuscript

NIH-PA Author Manuscript

to a direct pathophysiological consequence of PGC-1α underexpression on increased α-syn oligomerization. We speculate that insufficient function or underexpression of RG- or CNS-PGC-1α might predispose to α-syn aggregation, and could therefore be a potential risk factor for PD. Vice versa it is also possible that increased ROS production during aging leads to increased α-syn aggregation with a resulting downregulation of RG- or CNS-PGC-1α, which might further promote α-syn aggregation and toxicity.

Along the same line of evidence, a direct action of α-syn on the PGC-1α promoter has been reported, leading to PGC-1α repression [46]. An intriguing possibility would be that α-syn aggregates or oligomers bind more effectively to the promoter of PGC-1α than non-aggregated α-syn, thereby explaining the earlier down-regulation of different PGC-1α forms in the brainstem of transgenic A30P α-syn mice that is mostly and earliest affected by α-syn aggregates. Interestingly, also in HD downregulation of PGC-1α has been observed in human HD brain and in mouse striatum [55]. Several studies reported downregulation of PGC-1α mRNA with mutant huntingtin implicated in the transcription of PGC-1α [30, 84–87], whereas pharmacologic/transcriptional activation of PGC-1α had beneficial effects in models of HD [88–90].

Furthermore, in PD downregulation of the master regulator of mitochondrial biogenesis PGC-1α might be connected to the well characterized mitochondrial dysfunction observed in PD patients and respective experimental models [18, 20, 91–95]. Together, PGC-1α deregulation and α-syn aggregation are clearly negatively influencing each other which might also occur in the brains of PD patients leading to a vicious circle and potentially contribute to the etiology of PD.

In addition to our findings on PGC-1α deregulation on a transcriptional level, we also investigated whether restoration of PGC-1α function using both genetic and pharmacological approaches could rescue α-syn oligomerization and related toxicities. We found that RG-PGC-1α is capable of reducing α-syn oligomers and related toxicity. These results are in accordance with previous studies describing PGC-1α to be protective in the context of PD: PGC-1α increases the survival of neurons overexpressing the mutated A53T α-syn [47] and in the MPTP mouse model [96]. Furthermore, the repression of PGC-1α by PARIS kills dopaminergic neurons *in vivo*, and its reactivation prevents this loss [45]. Several mechanisms could underlie the observed protective effect of PGC-1α on α-syn oligomerization and toxicity. First, amelioration of mitochondrial function and reduction of ROS by PGC-1α could be beneficial, concerning α-syn-mediated toxicity, since overexpression of wild-type or mutant α-syn increases the rate of intracellular ROS [97, 98]. PGC-1α has already been shown to regulate the expression of ROS-detoxifying enzymes such as SOD2 and Gpx [30]. Thus, a direct effect of PGC-1α on ROS metabolism could explain the protective effect on α-syn-mediated toxicity. Second, beneficial effects of PGC-1α could be restoration of the PGC-1α target genes such as the subunits of complex I to V of the mitochondrial electron chain transport, genes involved in oxidative phosphorylation and mitochondrial biogenesis that are reduced in PD patients [43]. A third explanation for a protective effect of PGC-1α on α-syn oligomerization and toxicity might be through activation of the ALP. A recent study emphasized a role for PGC-1α in the elimination of huntingtin aggregation by activating the transcription factor EB (TFEB), a

NIH-PA Author Manuscript

NIH-PA Author Manuscript

NIH-PA Author Manuscript

master regulator of the ALP [31]. PGC-1α transactivation resulted in an enhanced ALP activity through the activation of TFEB. In our cell culture experiments, we observed an increase of the LC3 positive vesicles when PGC-1α is overexpressed together with αsyn. This increase of LC3 positive vesicles was accompanied by a decrease of αsyn oligomers. This reduction of α-syn oligomers could only be observed in cells with an intact ALP since treatment with ALP inhibitor BAF A1 abolished this effect. These results suggest that autophagy might be one potential, although possibly not the only mechanism involved in the PGC-1α dependent reduction of α-syn oligomers.

Furthermore, in midbrain dopamine neurons, TFEB activation has been shown to be directly inhibited by α-syn via blockage of nuclear translocation of TFEB leading to inhibition of the ALP [99]. However, the exact role of autophagy in this process warrants further investigation.

In conclusion, this study suggests that PGC-1α can ameliorate α-syn oligomerization and related toxicities. Insufficient function or underexpression of RG- or CNS-PGC-1α in the PD brain might accelerate α-syn oligomerization and contribute to neurodegenerative disease. Restoration of PGC-1α function might thus be a novel approach for the development of effective drugs for the treatment of PD and related synucleinopathies.

Supplementary Material

Refer to Web version on PubMed Central for supplementary material.

Acknowledgments

The excellent technical assistance of Ramona Langohr, Franziska Bachhuber and Kevin Letscher is gratefully acknowledged. This research was supported by funds from the Baustein Program Medical Faculty Ulm University (KMD, JE), the Virtual Helmholtz Institute “RNA dysmetabolism in ALS and FTD” of the DZNE (HB, AW, PW), Charcot Foundation (ACL, JHW), Alzheimer Forschung Initiative #13803 (DRT), BMBF (NGFN 01GS08134) (BL) and the FWF/DFG (LI 1745)(BL) and the National Institutes of Health (RO1-NS073740 to P.J.M and R01 NS065874 to A.R.L.).

References

1. Braak H, Del Tredici K, Rub U, de Vos RA, Jansen Steur EN, Braak E. Staging of brain pathology related to sporadic Parkinson’s disease. Neurobiol Aging. 2003 Mar-Apr;24(2):197–211. [PubMed: 12498954]
2. Goedert M. Alpha-synuclein and neurodegenerative diseases. Nat Rev Neurosci. 2001 Jul; 2(7): 492–501. [PubMed: 11433374]
3. El-Agnaf OM, Salem SA, Paleologou KE, et al. Detection of oligomeric forms of alpha-synuclein protein in human plasma as a potential biomarker for Parkinson’s disease. FASEB J. 2006 Mar; 20(3):419–25. [PubMed: 16507759]
4. Gosavi N, Lee HJ, Lee JS, Patel S, Lee SJ. Golgi fragmentation occurs in the cells with prefibrillar alpha-synuclein aggregates and precedes the formation of fibrillar inclusion. J Biol Chem. 2002 Dec 13; 277(50):48984–92. [PubMed: 12351643]
5. Kayed R, Head E, Thompson JL, et al. Common structure of soluble amyloid oligomers implies common mechanism of pathogenesis. Science. 2003 Apr 18; 300(5618):486–9. [PubMed: 12702875]
6. Lashuel HA, Hartley D, Petre BM, Walz T, Lansbury PT Jr. Neurodegenerative disease: amyloid pores from pathogenic mutations. Nature. 2002 Jul 18.418(6895):291. [PubMed: 12124613]

NIH-PA Author Manuscript NIH-PA Author Manuscript NIH-PA Author Manuscript

7. Masliah E, Rockenstein E, Veinbergs I, et al. Dopaminergic loss and inclusion body formation in alpha-synuclein mice: implications for neurodegenerative disorders. Science. 2000 Feb 18; 287(5456):1265–9. [PubMed: 10678833]
8. Danzer KM, Haasen D, Karow AR, et al. Different species of alpha-synuclein oligomers induce calcium influx and seeding. J Neurosci. 2007 Aug 22; 27(34):9220–32. [PubMed: 17715357]
9. Winner B, Jappelli R, Maji SK, et al. In vivo demonstration that alpha-synuclein oligomers are toxic. Proc Natl Acad Sci U S A. 2011 Mar 8; 108(10):4194–9. [PubMed: 21325059]
10. Auluck PK, Chan HY, Trojanowski JQ, Lee VM, Bonini NM. Chaperone suppression of alpha-synuclein toxicity in a Drosophila model for Parkinson's disease. Science. 2002 Feb 1; 295(5556): 865–8. [PubMed: 11823645]
11. Bodner RA, Outeiro TF, Altmann S, et al. Pharmacological promotion of inclusion formation: a therapeutic approach for Huntington's and Parkinson's diseases. Proc Natl Acad Sci U S A. 2006 Mar 14; 103(11):4246–51. [PubMed: 16537516]
12. Bucciantini M, Calloni G, Chiti F, et al. Prefibrillar amyloid protein aggregates share common features of cytotoxicity. J Biol Chem. 2004 Jul 23; 279(30):31374–82. [PubMed: 15133040]
13. Park JY, Lansbury PT Jr. Beta-synuclein inhibits formation of alpha-synuclein protofibrils: a possible therapeutic strategy against Parkinson's disease. Biochemistry. 2003 Apr 8; 42(13):3696–700. [PubMed: 12667059]
14. Abou-Sleiman PM, Muqit MM, Wood NW. Expanding insights of mitochondrial dysfunction in Parkinson's disease. Nat Rev Neurosci. 2006 Mar; 7(3):207–19. [PubMed: 16495942]
15. Banerjee R, Starkov AA, Beal MF, Thomas B. Mitochondrial dysfunction in the limelight of Parkinson's disease pathogenesis. Biochim Biophys Acta. 2009 Jul; 1792(7):651–63. [PubMed: 19059336]
16. Esteves AR, Arduino DM, Swerdlow RH, Oliveira CR, Cardoso SM. Oxidative stress involvement in alpha-synuclein oligomerization in Parkinson's disease cybrids. Antioxid Redox Signal. 2009 Mar; 11(3):439–48. [PubMed: 18717628]
17. Zhou C, Huang Y, Przedborski S. Oxidative stress in Parkinson's disease: a mechanism of pathogenic and therapeutic significance. Ann N Y Acad Sci. 2008 Dec.1147:93–104. [PubMed: 19076434]
18. Schapira AH, Cooper JM, Dexter D, Clark JB, Jenner P, Marsden CD. Mitochondrial complex I deficiency in Parkinson's disease. J Neurochem. 1990 Mar; 54(3):823–7. [PubMed: 2154550]
19. Spillantini MG, Schmidt ML, Lee VM, Trojanowski JQ, Jakes R, Goedert M. Alpha-synuclein in Lewy bodies. Nature. 1997 Aug 28; 388(6645):839–40. [PubMed: 9278044]
20. Lin MT, Beal MF. Mitochondrial dysfunction and oxidative stress in neurodegenerative diseases. Nature. 2006 Oct 19; 443(7113):787–95. [PubMed: 17051205]
21. Betarbet R, Sherer TB, MacKenzie G, Garcia-Osuna M, Panov AV, Greenamyre JT. Chronic systemic pesticide exposure reproduces features of Parkinson's disease. Nat Neurosci. 2000 Dec; 3(12):1301–6. [PubMed: 11100151]
22. Langston JW, Ballard PA Jr. Parkinson's disease in a chemist working with 1-methyl-4-phenyl-1,2,5,6-tetrahydropyridine. N Engl J Med. 1983 Aug 4.309(5):310. [PubMed: 6602944]
23. Sherer TB, Betarbet R, Kim JH, Greenamyre JT. Selective microglial activation in the rat rotenone model of Parkinson's disease. Neurosci Lett. 2003 May 1; 341(2):87–90. [PubMed: 12686372]
24. Zhang D, Anantharam V, Kanthasamy A, Kanthasamy AG. Neuroprotective effect of protein kinase C delta inhibitor rottlerin in cell culture and animal models of Parkinson's disease. J Pharmacol Exp Ther. 2007 Sep; 322(3):913–22. [PubMed: 17565007]
25. Betarbet R, Canet-Aviles RM, Sherer TB, et al. Intersecting pathways to neurodegeneration in Parkinson's disease: effects of the pesticide rotenone on DJ-1, alpha-synuclein, and the ubiquitin-proteasome system. Neurobiol Dis. 2006 May; 22(2):404–20. [PubMed: 16439141]
26. Schapira AH. Mitochondria in the aetiology and pathogenesis of Parkinson's disease. Lancet Neurol. 2008 Jan; 7(1):97–109. [PubMed: 18093566]
27. Sherer TB, Betarbet R, Stout AK, et al. An in vitro model of Parkinson's disease: linking mitochondrial impairment to altered alpha-synuclein metabolism and oxidative damage. J Neurosci. 2002 Aug 15; 22(16):7006–15. [PubMed: 12177198]

NIH-PA Author Manuscript NIH-PA Author Manuscript NIH-PA Author Manuscript

28. Thomas B, Beal MF. Parkinson's disease. Hum Mol Genet. 2007 Oct 15; 16(Spec No 2):R183–94. [PubMed: 17911161]
29. Puigserver P, Spiegelman BM. Peroxisome proliferator-activated receptor-gamma coactivator 1 alpha (PGC-1 alpha): transcriptional coactivator and metabolic regulator. Endocr Rev. 2003 Feb; 24(1):78–90. [PubMed: 12588810]
30. St-Pierre J, Drori S, Uldry M, et al. Suppression of reactive oxygen species and neurodegeneration by the PGC-1 transcriptional coactivators. Cell. 2006 Oct 20; 127(2):397–408. [PubMed: 17055439]
31. Tsunemi T, Ashe TD, Morrison BE, et al. PGC-1alpha rescues Huntington's disease proteotoxicity by preventing oxidative stress and promoting TFEB function. Sci Transl Med. 2012 Jul 11.4(142): 142ra97.
32. Ruas JL, White JP, Rao RR, et al. A PGC-1alpha isoform induced by resistance training regulates skeletal muscle hypertrophy. Cell. 2012 Dec 7; 151(6):1319–31. [PubMed: 23217713]
33. Soyal SM, Felder TK, Auer S, et al. A greatly extended PPARGC1A genomic locus encodes several new brain-specific isoforms and influences Huntington disease age of onset. Hum Mol Genet. 2012 Aug 1; 21(15):3461–73. [PubMed: 22589246]
34. Rona-Voros K, Weydt P. The Role of PGC-1alpha in the Pathogenesis of Neurodegenerative Disorders. Current drug targets. 2010 Jul 1.
35. Che HV, Metzger S, Portal E, Deyle C, Riess O, Nguyen HP. Localization of sequence variations in PGC-1alpha influence their modifying effect in Huntington disease. Mol Neurodegener. 2011; 6(1):1. [PubMed: 21211002]
36. Taherzadeh-Fard E, Saft C, Andrich J, Wieczorek S, Arning L. PGC-1alpha as modifier of onset age in Huntington disease. Mol Neurodegener. 2009; 4:10. [PubMed: 19200361]
37. Weydt P, Soyal SM, Gellera C, et al. The gene coding for PGC-1alpha modifies age at onset in Huntington's Disease. Mol Neurodegener. 2009; 4:3. [PubMed: 19133136]
38. Weydt P, Soyal SM, Landwehrmeyer GB, Patsch W. A single nucleotide polymorphism in the coding region of PGC-1alpha is a male-specific modifier of Huntington disease age-at-onset in a large European cohort. BMC neurology. 2014; 14:1. [PubMed: 24383721]
39. Ramos EM, Latourelle JC, Lee JH, et al. Population stratification may bias analysis of PGC-1alpha as a modifier of age at Huntington disease motor onset. Human genetics. 2012 Dec; 131(12):1833–40. [PubMed: 22825315]
40. Zhao W, Varghese M, Yemul S, et al. Peroxisome proliferator activator receptor gamma coactivator-1alpha (PGC-1alpha) improves motor performance and survival in a mouse model of amyotrophic lateral sclerosis. Mol Neurodegener. 2011; 6(1):51. [PubMed: 21771318]
41. Liang H, Ward WF, Jang YC, et al. PGC-1alpha protects neurons and alters disease progression in an amyotrophic lateral sclerosis mouse model. Muscle Nerve. 2011 Dec; 44(6):947–56. [PubMed: 22102466]
42. Eschbach J, Schwalenstocker B, Soyal SM, et al. PGC-1alpha is a male-specific disease modifier of human and experimental amyotrophic lateral sclerosis. Hum Mol Genet. 2013 Sep 1; 22(17): 3477–84. [PubMed: 23669350]
43. Zheng B, Liao Z, Locascio JJ, et al. PGC-1alpha, a potential therapeutic target for early intervention in Parkinson's disease. Sci Transl Med. 2010 Oct 6.2(52):52ra73.
44. Ciron C, Lengacher S, Dusonchet J, Aebischer P, Schneider BL. Sustained expression of PGC-1alpha in the rat nigrostriatal system selectively impairs dopaminergic function. Hum Mol Genet. 2012 Apr 15; 21(8):1861–76. [PubMed: 22246294]
45. Shin JH, Ko HS, Kang H, et al. PARIS (ZNF746) repression of PGC-1alpha contributes to neurodegeneration in Parkinson's disease. Cell. 2011 Mar 4; 144(5):689–702. [PubMed: 21376232]
46. Siddiqui A, Chinta SJ, Mallajosyula JK, et al. Selective binding of nuclear alpha-synuclein to the PGC1alpha promoter under conditions of oxidative stress may contribute to losses in mitochondrial function: implications for Parkinson's disease. Free Radic Biol Med. 2012 Aug 15; 53(4):993–1003. [PubMed: 22705949]

NIH-PA Author Manuscript NIH-PA Author Manuscript NIH-PA Author Manuscript

47. Wareski P, Vaarmann A, Choubey V, et al. PGC-1{alpha} and PGC-1{beta} regulate mitochondrial density in neurons. J Biol Chem. 2009 Aug 7; 284(32):21379–85. [PubMed: 19542216]
48. Kahle PJ, Neumann M, Ozmen L, Haass C. Physiology and pathophysiology of alpha-synuclein. Cell culture and transgenic animal models based on a Parkinson's disease-associated protein. Ann N Y Acad Sci. 2000; 920:33–41. [PubMed: 11193173]
49. Neumann M, Kahle PJ, Giasson BI, et al. Misfolded proteinase K-resistant hyperphosphorylated alpha-synuclein in aged transgenic mice with locomotor deterioration and in human alpha-synucleinopathies. J Clin Invest. 2002 Nov; 110(10):1429–39. [PubMed: 12438441]
50. Gomez-Isla T, Irizarry MC, Mariash A, et al. Motor dysfunction and gliosis with preserved dopaminergic markers in human alpha-synuclein A30P transgenic mice. Neurobiol Aging. 2003 Mar-Apr;24(2):245–58. [PubMed: 12498958]
51. Yavich L, Oksman M, Tanila H, et al. Locomotor activity and evoked dopamine release are reduced in mice overexpressing A30P-mutated human alpha-synuclein. Neurobiol Dis. 2005 Nov; 20(2):303–13. [PubMed: 16242637]
52. Leone TC, Lehman JJ, Finck BN, et al. PGC-1alpha deficiency causes multi-system energy metabolic derangements: muscle dysfunction, abnormal weight control and hepatic steatosis. PLoS Biol. 2005 Apr.3(4):e101. [PubMed: 15760270]
53. Danzer KM, Ruf WP, Putcha P, et al. Heat-shock protein 70 modulates toxic extracellular alpha-synuclein oligomers and rescues trans-synaptic toxicity. FASEB J. 2011 Jan; 25(1):326–36. [PubMed: 20876215]
54. Danzer KM, Kranich LR, Ruf WP, et al. Exosomal cell-to-cell transmission of alpha synuclein oligomers. Mol Neurodegener. 2012; 7:42. [PubMed: 22920859]
55. Weydt P, Pineda VV, Torrence AE, et al. Thermoregulatory and metabolic defects in Huntington's disease transgenic mice implicate PGC-1alpha in Huntington's disease neurodegeneration. Cell Metab. 2006 Nov; 4(5):349–62. [PubMed: 17055784]
56. Braunstein KE, Eschbach J, Rona-Voros K, et al. A point mutation in the dynein heavy chain gene leads to striatal atrophy and compromises neurite outgrowth of striatal neurons. Hum Mol Genet. 2010 Nov 15; 19(22):4385–98. [PubMed: 20807776]
57. Eschbach J, Fergani A, Oudart H, et al. Mutations in cytoplasmic dynein lead to a Huntington's disease-like defect in energy metabolism of brown and white adipose tissues. Biochim Biophys Acta. 2011 Jan; 1812(1):59–69. [PubMed: 20887786]
58. Schlaudraff F, Grundemann J, Fauler M, Dragicevic E, Hardy J, Liss B. Orchestrated increase of dopamine and PARK mRNAs but not miR-133b in dopamine neurons in Parkinson's disease. Neurobiol Aging. 2014 Oct; 35(10):2302–15. [PubMed: 24742361]
59. Rogers, GNWaCE. Symbolic Description of Factorial Models for Analysis of Variance. Journal of the Royal Statistical Society. 1973; 22(3):392–9.
60. Fassina L, Magenes G, Inzaghi A, et al. AUTOCOUNTER, an ImageJ JavaScript to analyze LC3B-GFP expression dynamics in autophagy-induced astrocytoma cells. Eur J Histochem. 2012; 56(4):e44. [PubMed: 23361240]
61. Freichel C, Neumann M, Ballard T, et al. Age-dependent cognitive decline and amygdala pathology in alpha-synuclein transgenic mice. Neurobiol Aging. 2007 Sep; 28(9):1421–35. [PubMed: 16872721]
62. Outeiro TF, Putcha P, Tetzlaff JE, et al. Formation of toxic oligomeric alpha-synuclein species in living cells. PLoS One. 2008; 3(4):e1867. [PubMed: 18382657]
63. Putcha P, Danzer KM, Kranich LR, et al. Brain-permeable small-molecule inhibitors of Hsp90 prevent alpha-synuclein oligomer formation and rescue alpha-synuclein-induced toxicity. J Pharmacol Exp Ther. 2010 Mar; 332(3):849–57. [PubMed: 19934398]
64. Remy I, Michnick SW. A highly sensitive protein-protein interaction assay based on Gaussia luciferase. Nat Methods. 2006 Dec; 3(12):977–9. [PubMed: 17099704]
65. Lagouge M, Argmann C, Gerhart-Hines Z, et al. Resveratrol improves mitochondrial function and protects against metabolic disease by activating SIRT1 and PGC-1alpha. Cell. 2006 Dec 15; 127(6):1109–22. [PubMed: 17112576]

NIH-PA Author Manuscript NIH-PA Author Manuscript NIH-PA Author Manuscript

66. Tadaishi M, Miura S, Kai Y, et al. Effect of exercise intensity and AICAR on isoform-specific expressions of murine skeletal muscle PGC-1alpha mRNA: a role of beta(2)-adrenergic receptor activation. Am J Physiol Endocrinol Metab. 2011 Feb; 300(2):E341–9. [PubMed: 21098736]

67. Price NL, Gomes AP, Ling AJ, et al. SIRT1 is required for AMPK activation and the beneficial effects of resveratrol on mitochondrial function. Cell Metab. 2012 May 2; 15(5):675–90. [PubMed: 22560220]

68. Dasgupta B, Milbrandt J. Resveratrol stimulates AMP kinase activity in neurons. Proc Natl Acad Sci U S A. 2007 Apr 24; 104(17):7217–22. [PubMed: 17438283]

69. Jager S, Handschin C, St-Pierre J, Spiegelman BM. AMP-activated protein kinase (AMPK) action in skeletal muscle via direct phosphorylation of PGC-1alpha. Proc Natl Acad Sci U S A. 2007 Jul 17; 104(29):12017–22. [PubMed: 17609368]

70. Canto C, Gerhart-Hines Z, Feige JN, et al. AMPK regulates energy expenditure by modulating NAD+ metabolism and SIRT1 activity. Nature. 2009 Apr 23; 458(7241):1056–60. [PubMed: 19262508]

71. Bain J, Plater L, Elliott M, et al. The selectivity of protein kinase inhibitors: a further update. Biochem J. 2007 Dec 15; 408(3):297–315. [PubMed: 17850214]

72. Desplats P, Lee HJ, Bae EJ, et al. Inclusion formation and neuronal cell death through neuron-to-neuron transmission of alpha-synuclein. Proc Natl Acad Sci U S A. 2009 Aug 4; 106(31):13010–5. [PubMed: 19651612]

73. Danzer KM, Krebs SK, Wolff M, Birk G, Hengerer B. Seeding induced by alpha-synuclein oligomers provides evidence for spreading of alpha-synuclein pathology. J Neurochem. 2009 Oct; 111(1):192–203. [PubMed: 19686384]

74. Luk KC, Song C, O'Brien P, et al. Exogenous alpha-synuclein fibrils seed the formation of Lewy body-like intracellular inclusions in cultured cells. Proc Natl Acad Sci U S A. 2009 Nov 24; 106(47):20051–6. [PubMed: 19892735]

75. Luk KC, Kehm V, Carroll J, et al. Pathological alpha-synuclein transmission initiates Parkinson-like neurodegeneration in nontransgenic mice. Science. 2012 Nov 16; 338(6109):949–53. [PubMed: 23161999]

76. Luk KC, Kehm VM, Zhang B, O'Brien P, Trojanowski JQ, Lee VM. Intracerebral inoculation of pathological alpha-synuclein initiates a rapidly progressive neurodegenerative alpha-synucleinopathy in mice. J Exp Med. 2012 May 7; 209(5):975–86. [PubMed: 22508839]

77. Hansen C, Angot E, Bergstrom AL, et al. alpha-Synuclein propagates from mouse brain to grafted dopaminergic neurons and seeds aggregation in cultured human cells. J Clin Invest. 2011 Feb; 121(2):715–25. [PubMed: 21245577]

78. Tritos NA, Mastaitis JW, Kokkotou EG, Puigserver P, Spiegelman BM, Maratos-Flier E. Characterization of the peroxisome proliferator activated receptor coactivator 1 alpha (PGC 1alpha) expression in the murine brain. Brain Res. 2003 Jan 31; 961(2):255–60. [PubMed: 12531492]

79. Lehman JJ, Barger PM, Kovacs A, Saffitz JE, Medeiros DM, Kelly DP. Peroxisome proliferator-activated receptor gamma coactivator-1 promotes cardiac mitochondrial biogenesis. J Clin Invest. 2000 Oct; 106(7):847–56. [PubMed: 11018072]

80. Russell LK, Mansfield CM, Lehman JJ, et al. Cardiac-specific induction of the transcriptional coactivator peroxisome proliferator-activated receptor gamma coactivator-1alpha promotes mitochondrial biogenesis and reversible cardiomyopathy in a developmental stage-dependent manner. Circ Res. 2004 Mar 5; 94(4):525–33. [PubMed: 14726475]

81. Miura S, Tomitsuka E, Kamei Y, et al. Overexpression of peroxisome proliferator-activated receptor gamma co-activator-1alpha leads to muscle atrophy with depletion of ATP. Am J Pathol. 2006 Oct; 169(4):1129–39. [PubMed: 17003473]

82. Bonen A. PGC-1alpha-induced improvements in skeletal muscle metabolism and insulin sensitivity. Appl Physiol Nutr Metab. 2009 Jun; 34(3):307–14. [PubMed: 19448691]

83. Rathke-Hartlieb S, Kahle PJ, Neumann M, et al. Sensitivity to MPTP is not increased in Parkinson's disease-associated mutant alpha-synuclein transgenic mice. J Neurochem. 2001 May; 77(4):1181–4. [PubMed: 11359883]

NIH-PA Author Manuscript NIH-PA Author Manuscript NIH-PA Author Manuscript

84. Chaturvedi RK, Adhihetty P, Shukla S, et al. Impaired PGC-1alpha function in muscle in Huntington's disease. Hum Mol Genet. 2009 Aug 15; 18(16):3048–65. [PubMed: 19460884]

85. Chaturvedi RK, Calingasan NY, Yang L, Hennessey T, Johri A, Beal MF. Impairment of PGC-1alpha expression, neuropathology and hepatic steatosis in a transgenic mouse model of Huntington's disease following chronic energy deprivation. Hum Mol Genet. 2010 Aug 15; 19(16):3190–205. [PubMed: 20529956]

86. Cui L, Jeong H, Borovecki F, Parkhurst CN, Tanese N, Krainc D. Transcriptional repression of PGC-1alpha by mutant huntingtin leads to mitochondrial dysfunction and neurodegeneration. Cell. 2006 Oct 6; 127(1):59–69. [PubMed: 17018277]

87. Johri A, Chandra A, Beal MF. PGC-1alpha, mitochondrial dysfunction, and Huntington's disease. Free Radic Biol Med. 2013 Sep.62:37–46. [PubMed: 23602910]

88. Chiang MC, Chen CM, Lee MR, et al. Modulation of energy deficiency in Huntington's disease via activation of the peroxisome proliferator-activated receptor gamma. Hum Mol Genet. 2010 Oct 15; 19(20):4043–58. [PubMed: 20668093]

89. Ho DJ, Calingasan NY, Wille E, Dumont M, Beal MF. Resveratrol protects against peripheral deficits in a mouse model of Huntington's disease. Exp Neurol. 2010 Sep; 225(1):74–84. [PubMed: 20561979]

90. Johri A, Calingasan NY, Hennessey TM, et al. Pharmacologic activation of mitochondrial biogenesis exerts widespread beneficial effects in a transgenic mouse model of Huntington's disease. Hum Mol Genet. 2012 Mar 1; 21(5):1124–37. [PubMed: 22095692]

91. Licker V, Turck N, Kovari E, et al. Proteomic analysis of human substantia nigra identifies novel candidates involved in Parkinson's disease pathogenesis. Proteomics. 2014 Mar; 14(6):784–94. [PubMed: 24449343]

92. Panov A, Dikalov S, Shalbuyeva N, Taylor G, Sherer T, Greenamyre JT. Rotenone model of Parkinson disease: multiple brain mitochondria dysfunctions after short term systemic rotenone intoxication. J Biol Chem. 2005 Dec 23; 280(51):42026–35. [PubMed: 16243845]

93. Pienaar IS, Elson JL, Racca C, Nelson G, Turnbull DM, Morris CM. Mitochondrial abnormality associates with type-specific neuronal loss and cell morphology changes in the pedunculopontine nucleus in Parkinson disease. Am J Pathol. 2013 Dec; 183(6):1826–40. [PubMed: 24099985]

94. Przedborski S, Tieu K, Perier C, Vila M. MPTP as a mitochondrial neurotoxic model of Parkinson's disease. Journal of bioenergetics and biomembranes. 2004 Aug; 36(4):375–9. [PubMed: 15377875]

95. Tufi R, Gandhi S, de Castro IP, et al. Enhancing nucleotide metabolism protects against mitochondrial dysfunction and neurodegeneration in a PINK1 model of Parkinson's disease. Nature cell biology. 2014 Feb; 16(2):157–66.

96. Mudo G, Makela J, Di Liberto V, et al. Transgenic expression and activation of PGC-1alpha protect dopaminergic neurons in the MPTP mouse model of Parkinson's disease. Cell Mol Life Sci. 2012 Apr; 69(7):1153–65. [PubMed: 21984601]

97. Hsu LJ, Sagara Y, Arroyo A, et al. alpha-synuclein promotes mitochondrial deficit and oxidative stress. The American journal of pathology. 2000 Aug; 157(2):401–10. [PubMed: 10934145]

98. Ono K, Yamada M. Antioxidant compounds have potent anti-fibrillogenic and fibril-destabilizing effects for alpha-synuclein fibrils in vitro. J Neurochem. 2006 Apr; 97(1):105–15. [PubMed: 16524383]

99. Decressac M, Mattsson B, Weikop P, Lundblad M, Jakobsson J, Bjorklund A. TFEB-mediated autophagy rescues midbrain dopamine neurons from alpha-synuclein toxicity. Proc Natl Acad Sci U S A. 2013 May 7; 110(19):E1817–26. [PubMed: 23610405]

NIH-PA Author Manuscript

NIH-PA Author Manuscript

NIH-PA Author Manuscript

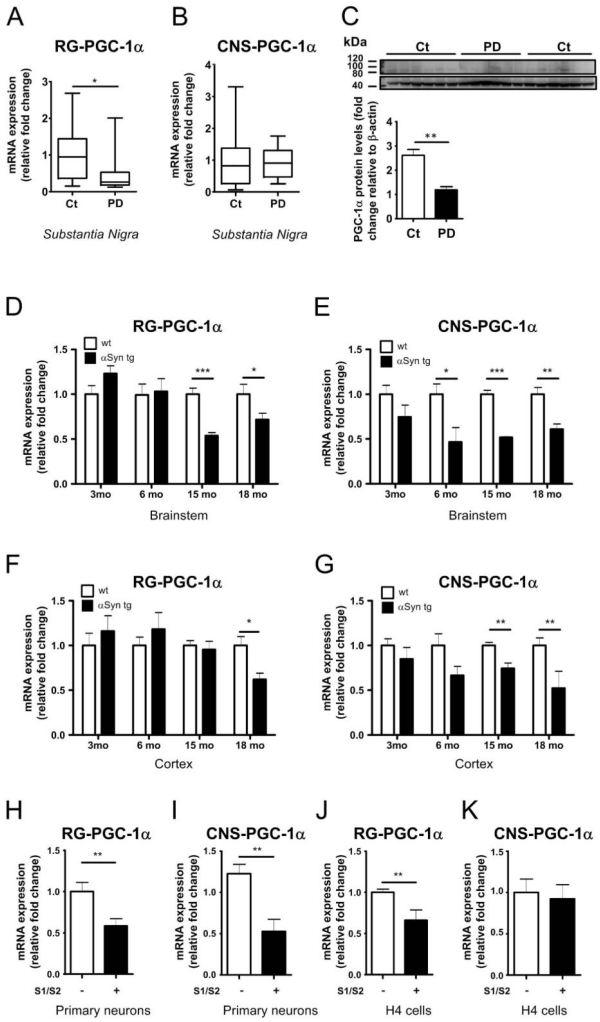

Figure 1. Decreased RG-PGC-1α and CNS-PGC-1α expression in PD patients, A30P-α-syn mice and in cell culture models for α-syn oligomerization

A. mRNA levels of RG-PGC-1α (A) and CNS-PGC-1α (B) in the *substantia nigra* of PD patients (PD) and non-PD controls (Ct). RG-PGC-1α and CNS-PGC-1α transcripts were normalized to POLR2A and TBP. PD n=10, Ct n=14. *p<0.05. **C.** Western Blot analysis of PGC-1α reveals reduced in PGC-1α levels in human tissue of SN of PD patients compared to non-PD controls. PD n=6, Ct n=10. Bar Graph represents the densitometric quantification of Western blots presented in panel C. **p<0.01. **D–E.** mRNA levels of RG-PGC-1α (D) and CNS-PGC-1α (E) in the brainstem of wild-type (+/+) and (Thy-1)-A30P-α-Synuclein mice at the indicated age (months). +/+ mice are in white columns, (Thy-1)-A30P-α-Synuclein mice in black columns. RG-PGC-1α and CNS-PGC-1α transcripts were normalized to POLR2A and TBP levels. *p<0.05, **p<0.01, ***p<0.005, n=4–6 animals per group. **F–G.** mRNA levels of RG-PGC-1α **(F)** and CNS-PGC-1α **(G)** in the cortex from wildtype (+/+) and (Thy-1)-A30P-α-Synuclein mice. mRNA transcripts were normalized to POLR2A and TBP levels, *p<0.05, **p<0.01, n=4–6 per group. +/+ mice are in white columns, (Thy-1)-A30P-α-Synuclein mice in black columns. **H–I.** mRNA levels of RG-PGC-1α **(H)** and CNS-PGC-1α **(I)** in wild-type primary neurons co-infected with AAV-S1/

NIH-PA Author Manuscript

NIH-PA Author Manuscript

NIH-PA Author Manuscript

AAV-S2 or control for 3 days. Four independent experiments were performed. mRNA transcripts were normalized to POLR2A and TBP levels. **p<0.01. **(J)** mRNA levels of RG-PGC-1α in H4 transiently co-transfected with S1/S2 for 48h. Three independent experiments were performed. **p<0.01. **(K)** mRNA levels of CNS-PGC-1 in H4 transiently co-transfected with S1/S2 for 48h. Three independent experiments were performed. mRNA levels were standardized using POLR2A and TBP levels.

NIH-PA Author Manuscript
NIH-PA Author Manuscript
NIH-PA Author Manuscript

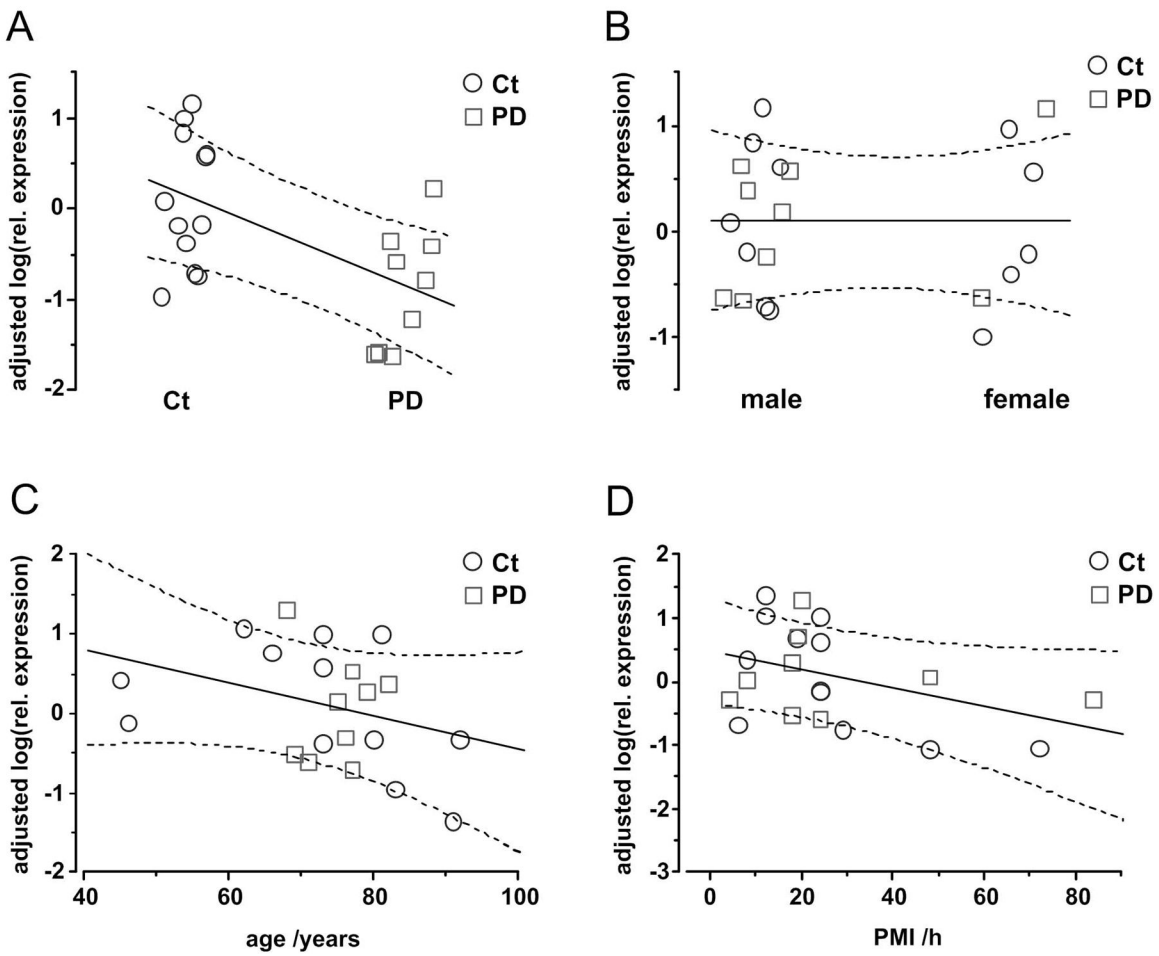

Figure 2. Adjusted effects on relative expression of RG-PGC-1α

Isolated effects of the variables disease group, gender, age and PMI are displayed as predicted by the linear mixed effects model. Only the presence of PD **(A)** had a significant effect on rel. expression values (see also Supplementary Table 1). Neither gender **(B)**, age **(C)** or PMI **(D)** had any relevant influence on RG-PCG1α expression. Shown are the adjusted relative expression values. These values are controlled for the influence by all random and fixed effects in the model except the one that is selected as the independent variable (on the x-axis). Solid and dashed lines represent marginal predictions with their 5–95% confidence bands. Control samples are shown as blue circles, PD samples as red squares.

NIH-PA Author Manuscript

NIH-PA Author Manuscript

NIH-PA Author Manuscript

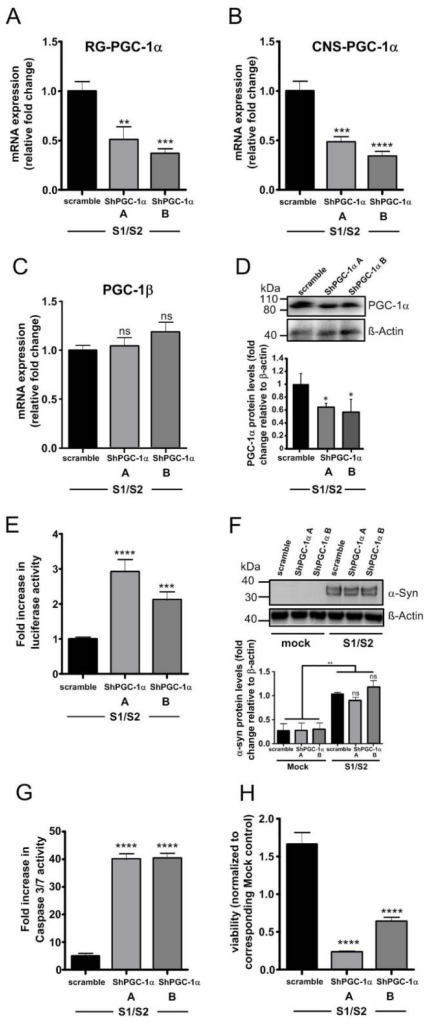

Figure 3. RG-and CNS-PGC-1α knockdown increases α-syn oligomerization and resulting toxicity

(A) RT-qPCR analysis of RG-PGC-1α from H4 cells co-transfected with S1/S2 and the two independent ShRNAs (ShPGC-1α-A and ShPGC-1α-B.). mRNA levels were standardized using POLR2A and TBP. A total of four independent experiments were performed. *p<0.05, **p<0.01, ***p<0.005. (**B)** RT-qPCR analysis of CNS-PGC-1α from H4 cells co-transfected with S1/S2 and the two independent ShRNAs (ShPGC-1α-A and ShPGC-1α-B). mRNA levels were standardized using POLR2A and TBP. A total for four independent experiments were performed. *p<0.05, **p<0.01, ***p<0.005. **(C)** RT-qPCR analysis of PGC-1β from H4 cells co-transfected with S1/S2 and the two independent ShRNAs (ShPGC-1α-A and ShPGC-1α-B). mRNA levels were standardized using POLR2A and TBP. A total of three independent experiments were performed showing that PGC-1β expression is not affected by PGC-1α ShRNAs. **(D)** Representative Western blotting showing PGC-1α and β-actin levels. PGC-1α levels are reduced in H4 cells co-transfected with S1/S2 and the two independent ShRNAs (ShPGC-1α-A and ShPGC-1α-B). Bar Graph represents the densitometric quantification of Western blots, n=3, *p<0.05. **(E)** Luciferase assay from H4 cells 24h post-infection with indicated lenti-shRNAs and co-transfection with

NIH-PA Author Manuscript

NIH-PA Author Manuscript

NIH-PA Author Manuscript

S1/S2. Six independent experiments were performed. ***p<0.005. ****p<0.001. **(F)** Representative Western blots showing α-syn and β-actin levels from H4 cells co-transfected with S1/S2 and the two independent ShRNAs (ShPGC-1α-A and ShPGC-1α-B). Bar Graph represents the densitometric quantification of Western blots, n=4, **p<0.01. Note that equal amounts of S1/S2 are produced in both Sh-scramble and ShPGC-1α conditions. **(G)** H4 cells 24h post-infection with indicated lenti-shRNAs and co-transfection with S1/S2 were assayed for Caspase 3–7 activity. A total for three experiments were performed. ***p<0.005, ****p<0.001. **(H)** 24h post-infection with indicated lenti-shRNAs and co-transfection with S1/S2 cytotoxicity was assessed in H4 cells using the cell titer glow assay which measures ATP levels in cells. Values are normalized to respective mock controls. ShPGC-1a A and ShPGC1a B are presented in relation to the Sh-scramble control. A total for three independent experiments were performed,***p<0.005, ****p<0.001.

NIH-PA Author Manuscript

NIH-PA Author Manuscript

NIH-PA Author Manuscript

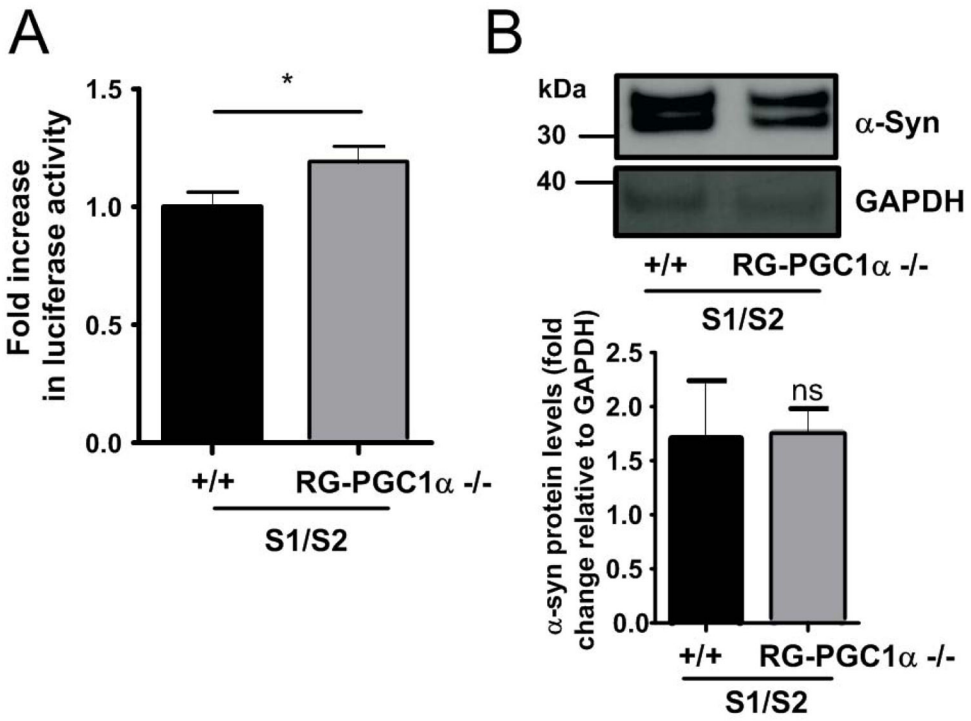

Figure 4. PGC-1α deficiency increases α-syn oligomerization in cortical primary neurons

(A) Luciferase assay from wildtype (+/+) and RG-PGC-1α −/− primary neurons incubated for 72h with AAV-S1and AAV-S2. Six independent experiments were performed, * $p<0.05$

(B) Representative Western blotting showing α-syn and GAPDH levels. Bar Graph represents the densitometric quantification of Western blots, n=3. ns=not significant. Note that equal amounts of S1/S2 are produced in both +/+ and RG-PGC-1α −/− primary neurons.

NIH-PA Author Manuscript

NIH-PA Author Manuscript

NIH-PA Author Manuscript

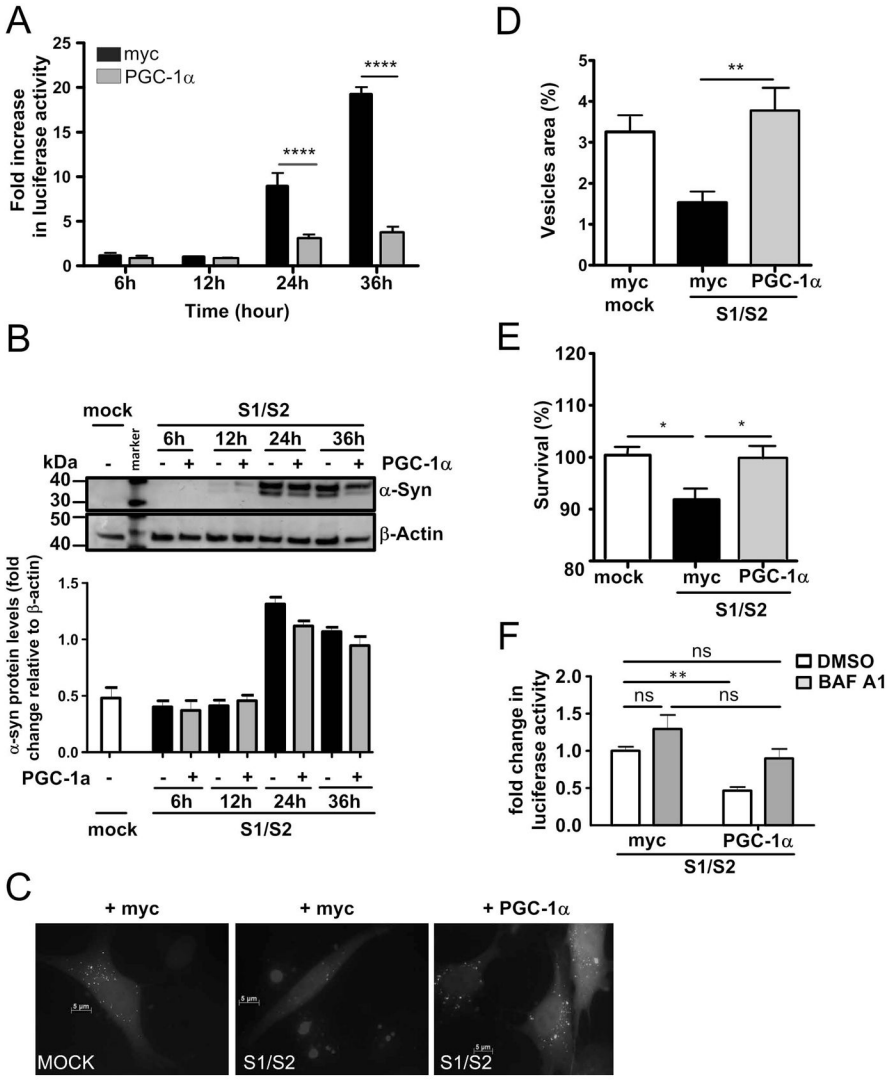

Figure 5. Restoration of PGC-1α reduces α-syn oligomerization and α-syn-mediated toxicity in H4 cells

(A) Luciferase assay from H4 cells transiently co-transfected with S1/S2 together with control plasmid myc (black column) or vector encoding RG-PGC-1α (grey column) for the indicated time. Four independent experiments were performed ****p<0.0001. **(B)** Representative Western blot shows α-syn and β-actin levels. Bar Graph represents the densitometric quantification of Western blots, n=3**. (C)** Immunofluorescence analysis of LC3 morphology in H4 cells transiently co-transfected S1/S2 or mock together with the control plasmid myc or vector encoding the RG-PGC-1α together with the LC3 Premo™ Autophagy Sensors (LC3B-GFP in green). **(D)** Quantification of LC3-positive vesicles using the ImageJ pluggin "autocounter". Results were standardized according the cell surface, *p<0.05. **(E)** 24h post co-transfection with S1/S2 and control plasmid myc or RG- PGC-1α plasmid cytotoxicity was assessed in H4 cells using the cell titer glow assay which measures ATP levels in cells. A total for three experiments were performed, *p<0.05. **(F)** Luciferase assay from H4 cells co-transfected with S1/S2 together with control plasmid myc or vector

encoding RG-PGC-1α treated with DMSO (white columns) or 200 nM BAF A1 (grey columns) for 20h. Data were pooled from n=3 independent experiments, **p<0.01, ns=not significant.

NIH-PA Author Manuscript
NIH-PA Author Manuscript
NIH-PA Author Manuscript

NIH-PA Author Manuscript

NIH-PA Author Manuscript

NIH-PA Author Manuscript

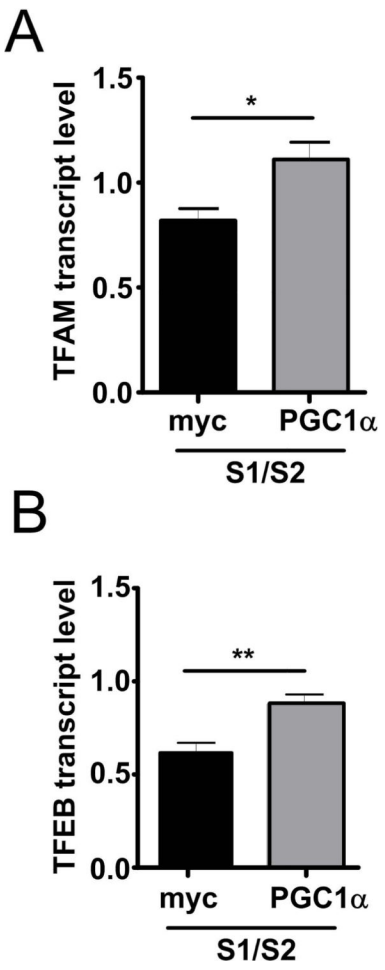

Figure 6. PGC-1α overexpression restores the expression levels of PGC-1α target genes upon α-Synuclein overexpression

mRNA levels of PGC-1α target genes TFAM **(A)** or transcription factor EB (TFEB) **(B)** in H4 co-transfected with S1/S2 for 48h together with myc-control plasmid (black column) or vector encoding RG-PGC-1α (grey columns). mRNA levels were standardized using POLR2A and TBP $^{**}p < 0.01$, $^{*}p<0.05$.

NIH-PA Author Manuscript

NIH-PA Author Manuscript

NIH-PA Author Manuscript

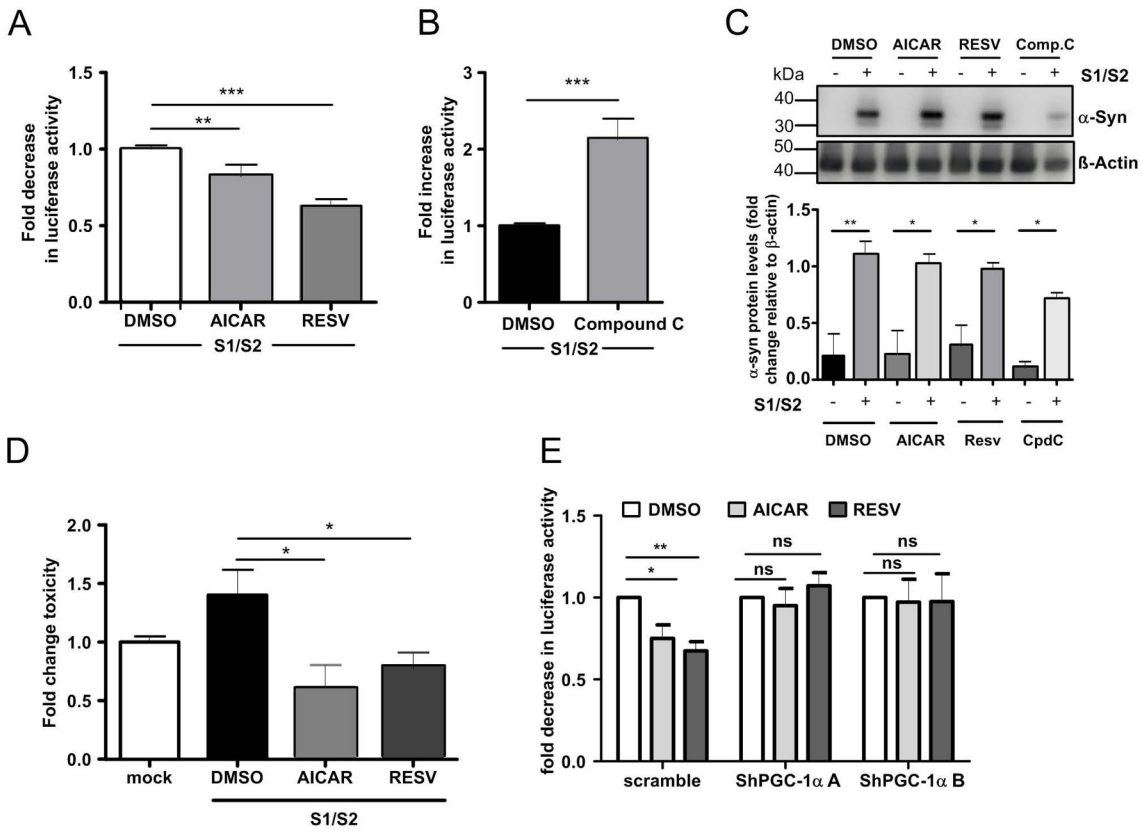

Figure 7. Pharmacological activation of PGC-1α decreases α-syn oligomerization *in vitro*.

A. Luciferase assay from H4 cells co-transfected with S1/S2 for 16h and then treated with 20μM Resveratrol or 1mM AICAR for 24 hours, n=10, **p<0.05. **(B)** Luciferase activity assay from H4 cells co-transfected with S1/S2 for 16h and then treated with 2μM compoundC for 24 hours, n=10, ***p<0.001 **(C)** Representative Western blots showing α-syn and β-actin levels. Bar Graph represents the densitometric quantification of Western blots, n=3, *p<0.05, **p<0.01. **(D)** H4 cells co-transfected with S1/S2 for 16h and then treated with 20μM Resveratrol, 1mM AICAR or 2μM compoundC for 24 hours. Cytotoxicity was assessed in H4 cells using the Caspase 3/7 activity assay. A total of three independent experiments was performed, values were normalized to respective mock controls, *p<0.05. **(E)** Luciferase assay from H4 cells post-infection with indicated lenti-shRNAs and co-transfection with S1/S2 for 16h, then treated with 20μM Resveratrol or 1mM AICAR for 24 hours. Values are normalized to respective DMSO controls. Data are represented as pooled data from n=7 independent experiments. *p<0.05. **p<0.01.

NIH-PA Author Manuscript

NIH-PA Author Manuscript

NIH-PA Author Manuscript

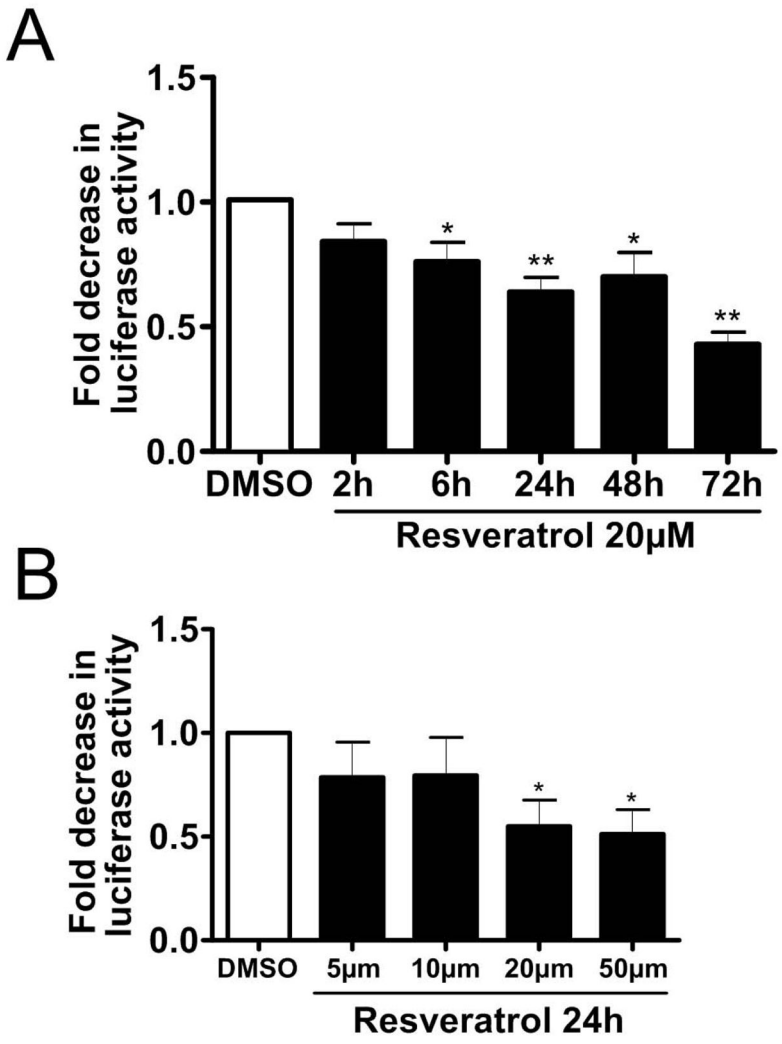

Figure 8. Resveratrol treatment decreases α-Synuclein oligomerization

(A) Luciferase assay from H4 cells co-transfected with S1/S2 and treated with 20μM resveratrol for the indicated time periods, ** $p<0.01$, ***$p<0.005$, n=6. (**B)** Luciferase assay from H4 cells co-transfected with S1/S2 and treated for 24h at the indicated resveratrol concentrations, * $p<0.05$, n=8.

NIH-PA Author Manuscript

NIH-PA Author Manuscript

NIH-PA Author Manuscript

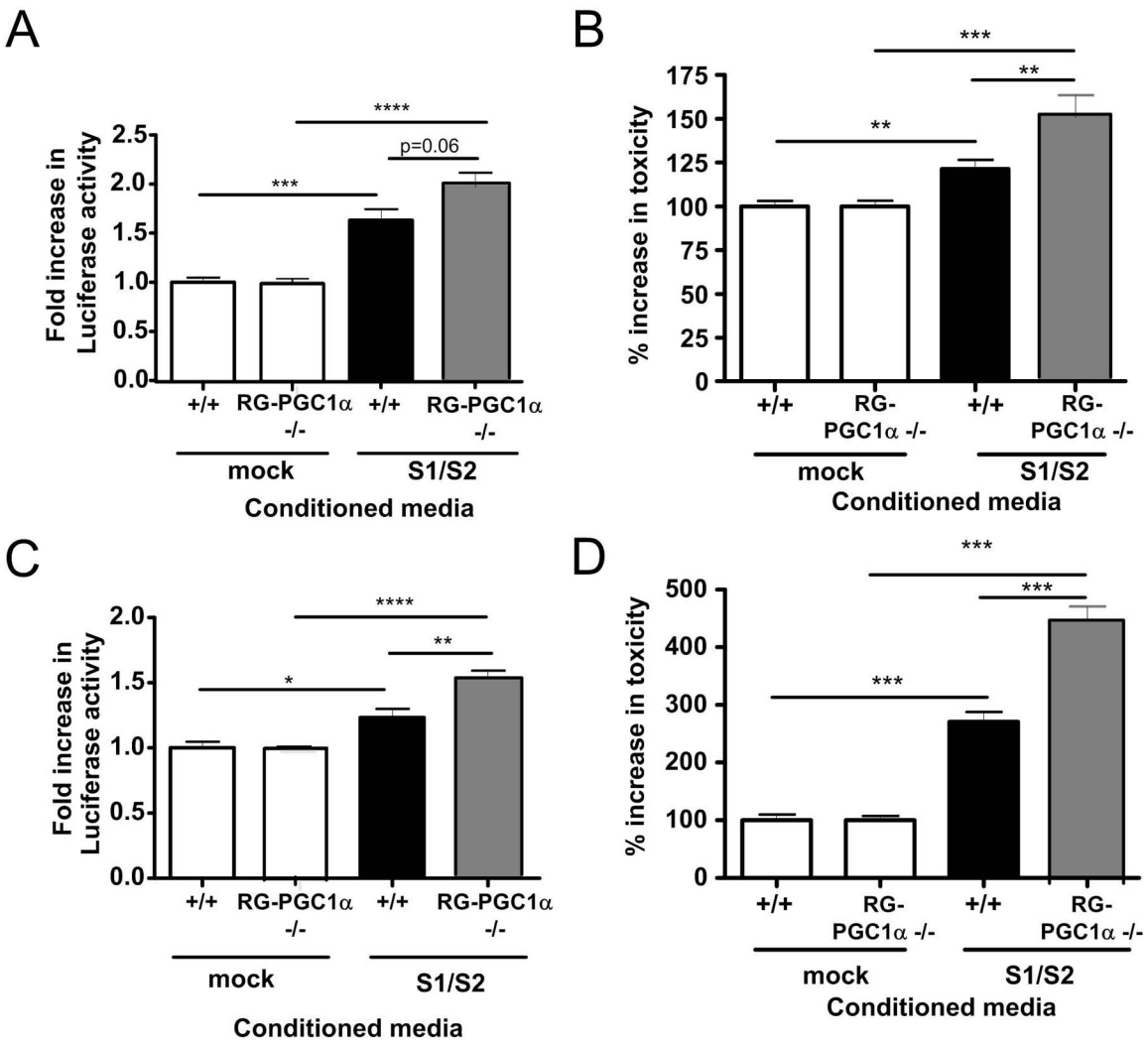

Figure 9. RG-PGC-1α deficiency in primary neurons increases α-syn oligomer accumulation and toxicity

(A) Luciferase assay from wildtype (+/+) or RG-PGC-1α −/− primary neurons incubated for 48h with conditioned media from H4 cells transfected with mock or S1/S2, *p<0.05, **p<0.01, ***p<0.001, n=3. **(B)** Primary neurons from +/+ or RG-PGC-1α −/− mice were assayed for release of adenylate kinase using the ToxiLight™ assay after 48h incubation with conditioned media from H4 cells transfected with mock or S1/S2. Three independent experiments were performed, *p<0.05, **p<0.01, ***p<0.001. **(C)** Luciferase assay from +/+ or RG-PGC-1α −/− primary neurons incubated for 72h with conditioned media from H4 cells transfected with mock or S1/S2, n=3, **p<0.01, ***p<0.001. **(D)** Primary neurons from +/+ or RG-PGC-1α −/− mice were assayed for release of adenylate kinase using the ToxiLight™ assay after 72h incubation with conditioned media from H4 cells transfected with mock or S1/S2. Three independent experiments were performed, *p<0.05, **p<0.01, ***p<0.001.

NIH-PA Author Manuscript NIH-PA Author Manuscript NIH-PA Author Manuscript

Ann Neurol. Author manuscript; available in PMC 2016 January 01.

TABLE 1

Characteristics of human cases

ID	gender	age	PMI [h]	co-morbidities, agonal factors	cause of death	PD Braak stage
PD #1	m	77	24	dementia	myocardiac infarct	5
PD #2	m	79	48	depression, Binswanger's disease	embolism of the arteries of the lungs	6
PD #3	m	82	84	no	broncopneumonia, sepsis	5
PD #4	m	71	18	dementia	broncopneumonia, sepsis	5
PD #5	m	75	18	dementia	broncopneumonia, sepsis	5
PD #6	m	76	8	dementia	coronary disease	5
PD #7	f	68	20	N/K	N/K	5
PD #8	f	69	n.k.	N/K	respiratory arrest due to high aspiration	5
PD #9	f	71	n.k.	N/K	N/K	5
PD #10	m	77	19	severe depression	respiratory arrest	6

ID	gender	age	PMI [h]	co-morbidities, agonal factors	cause of death	PD Braak stage
Control #1	m	81	12	no	N/K	N/A
Control #2	f	91	6	prior minor stroke	N/K	N/A
Control #3	f	73	72	no	N/K	N/A
Control #4	m	92	8	Binswanger's disease	N/K	N/A
Control #5	m	66	24	no	sepsis after small intestine perforation	N/A
Control #6	m	45	24	no	myocardial infarct	N/A
Control #7	m	46	29	no	heart failure	N/A
Control #8	f	73	24	plasmocytome	not known	N/A
Control #9	m	83	48	arterial hypertension	myocardial infarct	N/A
Control #10	m	62	12	cancer	cirrhosis of the liver	N/A
Control #11	f	80	24	hypertonic arteriopathy	heart failure	N/A
Control #12	f	73	19	N/K	N/K	N/A
Control #13	f	72	n.k.	N/K	N/K	N/A
Control #14	f	74	n.k.	N/K	N/K	N/A

The table summarizes the characteristics of PD patients and controls from Ulm University, University of California San Diego and Mayo Clinic Jacksonville who have come to post mortem. N/K= not known; N/A=not applicable, PMI=post mortem interval